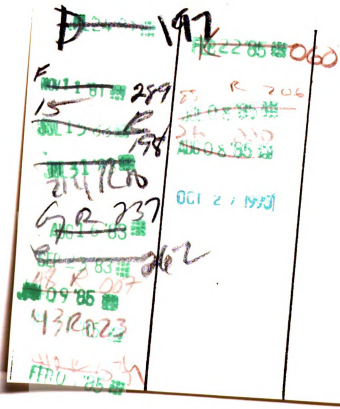




OVERDUE FINES: 25¢ per day per item

RETURNING LIBRARY MATERIALS:

Place in book return to remove charge from circulation records



## GASIFICATION OF POPLAR SPP CHAR

Ву

Craig Anderson

## A THESIS

Submitted to
Michigan State University
in partial fulfillment of the requirements
for the degree of

MASTER OF SCIENCE

Department of Chemical Engineering

#### ABSTRACT

### GASIFICATION OF POPLAR SPP CHAR

By

## Craig Anderson

A study has been made of the gasification of wood char. To produce the char, Poplar SPP was pyrolyzed in nitrogen at 700°C for 10 minutes. The rate of gasification was measured at temperatures of 550°C, 625°C, and 685°C, at steam partial pressures of 46 kPa to 100 kPa, and for space velocities of 2.0 s<sup>-1</sup> to 7.3 s<sup>-1</sup>. It was not certain if the methane was formed directly from the char or from the carbon monoxide in the product gas so the gasification rate was calculated for two cases.

In Case I the gasification rate was calculated from the carbon in the carbon oxides of the product gas. The following gasification rate expression was found.

rate = 
$$k_0 \exp(-E_a/RT)$$
  $p_{H_2O} \frac{\text{moles of carbon consumed}}{\text{min gram of original carbon}}$ 

In Case II the gasification rate was calculated from the carbon in the carbon oxides and the methane.

The gasification rate expression was found to be the following.

$$rate = \frac{k_1 p_{H_2O}}{1 + k_2 p_{H_2O}} \frac{moles of carbon consumed}{min gram of original carbon}$$

Wood is composed of basically two different sized cells with inner radii of 35  $\mu m$  and 10  $\mu m$ . An isothermal effectiveness factor for particles of wood is essentially that of the smaller cells. The model predicted that diffusion control becomes important for particles larger than 0.5 cm at 625°C.

### **ACKNOWLEDGEMENTS**

The author would like to express his appreciation to his academic advisor, Dr. Martin C. Hawley for his guidance and assistance. Appreciation is also given to Mr. Mark Boyd for his assistance and cooperation in carrying out the research experiments. The advice of Dr. John E. Young for setting up the laboratory is also appreciated. The microphotographs were made by Mr. Robert Konopacz.

# TABLE OF CONTENTS

|     |     |            |                  |           |          |     |      |      |      |     |     |    |   |   |   |   |   | Page                 |
|-----|-----|------------|------------------|-----------|----------|-----|------|------|------|-----|-----|----|---|---|---|---|---|----------------------|
| LIS | ST  | OF         | TAB              | LES       | <b>;</b> | •   | •    | •    | •    | •   | •   | •  | • | • | • | • | • | iv                   |
| LIS | ST  | OF         | FIG              | URE       | S        | •   | •    | •    | •    | •   | •   | •  | • | • | • | • | • | v                    |
| LIS | ST  | OF         | SYM              | воі       | S        | •   | •    | •    | •    | •   | •   | •  | • | • | • | • | • | vii                  |
| IN  | ro  | DUC        | TIO              | N         | •        | •   | •    | •    | •    | •   | •   | •  | • | • | • | • | • | 1                    |
| BA  | CKG | ROU        | IND              | •         | •        | •   | •    | •    | •    | •   | •   | •  | • | • | • | • | • | 3                    |
| EXI | PER | IME        | ENTA             | L A       | PPA      | RAI | US   | AND  | ) PR | OCE | DUF | ES | • | • | • | • | • | 19                   |
| 9   | Sam | ple<br>rat | tus<br>Pr<br>ing | epa<br>Pr | oce      |     | :e   | •    |      | •   | •   | •  | • | • | • | • | • | 19<br>23<br>24<br>29 |
|     | SUL |            | •                | •         | •        | •   | •    | •    | •    | •   | •   | •  | • | • | • | • | • | 31                   |
| DIS | SCU | SSI        | ON               | OF        | EXE      | ERI | MEN  | TAI  | RE   | SUL | TS  | •  | • | • | • | • | • | 41                   |
| 1   |     | or         | cs<br>Ana<br>bri |           |          |     | lera | itic | ons  | •   | •   | •  | • | • |   | • | • | 41<br>45<br>47       |
| MOI | DEL | INC        | 3                | •         | •        | •   | •    | •    | •    | •   | •   | •  | • | • |   | • | • | 53                   |
| CO  | NCL | usi        | ONS              | 3         | •        | •   | •    | •    | •    | •   | •   | •  | • | • | • | • | • | 60                   |
| RE  | СОМ | MEN        | IDAT             | OI        | IS       | •   | •    | •    | •    | •   | •   | •  | • | • | • | • | • | 63                   |
| AP  | PEN | DIX        | ζ                | •         | •        | •   | •    | •    | •    | •   | •   | •  | • | • | • | • | • | 65                   |
| RE  | FER | ENC        | ES               | •         | •        | •   | •    | •    | •    | •   | •   | •  |   | • | • | • |   | 69                   |

# LIST OF TABLES

| <b>Table</b> |                                                                                                                                               | Page |
|--------------|-----------------------------------------------------------------------------------------------------------------------------------------------|------|
|              | Dispersion of second the medical                                                                                                              |      |
| ⊥•           | Elemental analysis of coconut char produced in nitrogen at 950°C                                                                              | 12   |
| 2.           | Summary of gasification rate results for varying space velocities at 625°C and steam partial pressure of 100 kPa                              | 32   |
| 3.           | Summary of gasification rate results for varying steam partial pressures at 625°C and space velocity of 4 s-1                                 | 33   |
| 4.           | Summary of gasification rate results for varying temperatures at steam partial pressure of 100 kPa and space velocity of 4 s-1                | . 34 |
| 5.           | Average outlet gas compositions for the space velocity experiments at 625°C and steam partial pressure of 100 kPa                             |      |
| 6.           | Average outlet gas compositions for the steam partial pressure experiments at 625°C and space velocity of 4 s <sup>-1</sup>                   | . 51 |
| 7.           | Average outlet gas compositions for the temper ature experiments at steam partial pressure of 100 kPa and space velocity of 4 s <sup>-1</sup> |      |

# LIST OF FIGURES

| Figur | е                                                                                                                                                           | Page |
|-------|-------------------------------------------------------------------------------------------------------------------------------------------------------------|------|
| 1.    | Chemical structure of cellulose                                                                                                                             | 4    |
| 2.    | Chemical structure of lignin                                                                                                                                | 5    |
| 3.    | Microphotograph of Poplar SPP at 200 magnification                                                                                                          | 7    |
| 4.    | Schematic diagram of gasification apparatus .                                                                                                               | 20   |
| 5.    | Photograph of gasification reactor                                                                                                                          | 21   |
| 6.    | Photograph of gasification apparatus                                                                                                                        | 21   |
| 7.    | Pyrolysis weight loss versus pyrolysis time for Poplar SPP in nitrogen at 700°C                                                                             | 25   |
| 8.    | Microphotograph of Poplar SPP before and after pyrolysis                                                                                                    | 26   |
| 9.    | Gasification rate of Poplar SPP char versus space velocity at 625°C and steam partial pressure of 100 kPa                                                   | 35   |
| 10.   | Gasification rate of Poplar SPP char versus steam partial pressure at 625°C and space velocity of 4 s <sup>-1</sup> (Case I)                                | 38   |
| 11.   | Gasification rate of Poplar SPP char versus steam partial pressure at 625°C and space velocity of 4 s <sup>-1</sup> (Case II)                               | 39   |
| 12.   | Natural log of gasification rate (mol/g min) of Poplar SPP char versus inverse temperature at steam partial pressure of 100 kPa and space velocity of 4 s-1 | 40   |
| 13.   | Equilibrium mole fractions as a function of temperature for a steam-carbon system at a total pressure of 101 kPa                                            | 48   |

| Figur | e P                                                                                             | age |
|-------|-------------------------------------------------------------------------------------------------|-----|
| 14.   | Diagram of model cell                                                                           | 54  |
| 15.   | Isothermal effectiveness factor versus cell length for gasification of Poplar SPP char at 625°C | 59  |

## LIST OF SYMBOLS

c, c<sub>o</sub> = steam concentration in cell, in bulk fluid, mol/cm<sup>3</sup>

 $E_a = activation energy, kJ$ 

 $f_i$  = gas chromatograph correlation factor

j; = adsorption-desorption constants

k = rate constant, mol/g min kPa

k' = rate constant, cm<sup>3</sup>/g sec

k<sub>1</sub> = rate constant, mol/g min kPa

 $k_2$  = rate constant,  $kPa^{-1}$ 

 $k_3$  = rate constant, mol/g min kPa<sup>2</sup>

L = length of model cell, cm

 $\ell = \frac{1}{2}L$ , cm

 $P_{H_2O}$  = partial pressure of steam, kPa

P<sub>H2</sub> = partial pressure of hydrogen, kPa

r, r<sub>o</sub> = inner radius of model cell, initial inner radius, cm

R = outer radius of model cell, cm

 $R_0 = R^2 - r_0^2 + c_0^2$ 

T = temperature

t = time, s

w; = weight of gas chromatograph peak

x = axial coordinate of model cell, cm

# **Greek Letters**

- $\xi$  = dimensionless length = x/1
- $\eta$  = isothermal effectiveness factor
- $\psi$  = dimensionless concentration = c/c<sub>o</sub>

$$\phi = \sqrt{(R_0 \rho k' l^2/r^2 D)}$$

 $\rho$  = density of graphite, g/cm<sup>3</sup>

### INTRODUCTION

Gasification of biomass and coal is a research area that is currently receiving a large amount of attention. In gasification steam is added as a reactant whereas in pyrolysis thermal degradation of the biomass occurs in an inert atmosphere. The gasification products, called synthesis gas, are hydrogen, carbon monoxide, carbon dioxide, and methane. The product gas can be burned directly and used as an energy source or as a feedstock for producing desired hydrocarbons.

This study presents an experimental method for studying the gasification reaction of biomass. The results are used to determine the intrinsic kinetics of the gasification reaction. Using this information a mathematical model is developed to predict the results which would be obtained by using different sample sizes.

The initial objective of this work was to study the gasification of dried wood. In preliminary experiments when dried wood was reacted with steam at high temperature both pyrolysis and gasification occurred. Pyrolysis products, which include tars, could not be analyzed in our laboratory. In order to separate the

two processes, gasification and pyrolysis, it was decided to study gasification of wood char at various steam partial pressures, temperatures, and space velocities so the gasification kinetics could be determined separately from pyrolysis.

Char samples were made by pyrolyzing Poplar SPP encironart? at 700°C for 10 minutes. Poplar SPP was selected based on discussions with Dr. J. W. Hanover of the Michigan State University, Department of Forestry. This species of wood is fast growing and is currently considered as a prime candidate for large scale production on a "biomass plantation."

The experimentation was a joint effort with Mr. M. R. Boyd. The overall experimental study included both catalyzed and uncatalyzed gasification of char. This study presents only the results of noncatalytic gasification using untreated char. Mr. Boyd presents results using char treated with potassium carbonate and sodium carbonate to catalyze the gasification reaction.

### **BACKGROUND**

Chemically, wood is composed primarily of cellulose, hemicellulose, lignin, and water. The relative amounts of each material vary with different species of wood. On a water free basis, hardwoods contain between 75% to 82% total cellulose and softwoods contain 70% to 75% total cellulose (1). The remainder is essentially lignin with 1% to 2% of the wood being ash and extractives. Poplar is a hardwood and has a composition of 48.8% cellulose, 29.7% hemicellulose, 19.3% lignin, and the rest is ash and extractives (2). Cellulose is a polymer composed of repeating glucosan units and the chemical structure is shown in Figure 1. Hemicellulose is composed of two classes of materials: xylans and glucomannans. Xylans are polymers made from pentose sugars and glucomannans are polymers made from hexose sugars. Lignin is not a single compound but is a mixture of various compounds. It is made of repeating C<sub>6</sub>-C<sub>3</sub> units with ether linkages and is virtually noncrystalline. example of the chemical structure of lignin is shown in Figure 2.

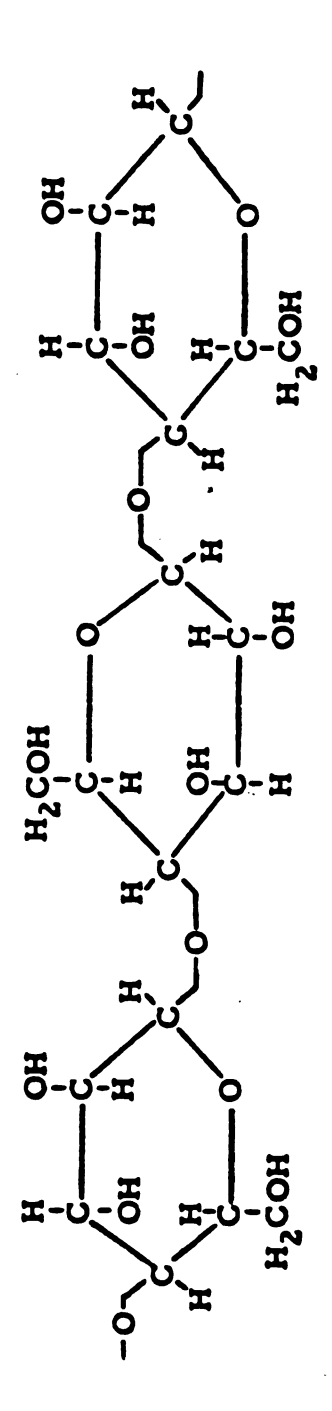


Figure 1. -- Chemical Structure of Cellulose.

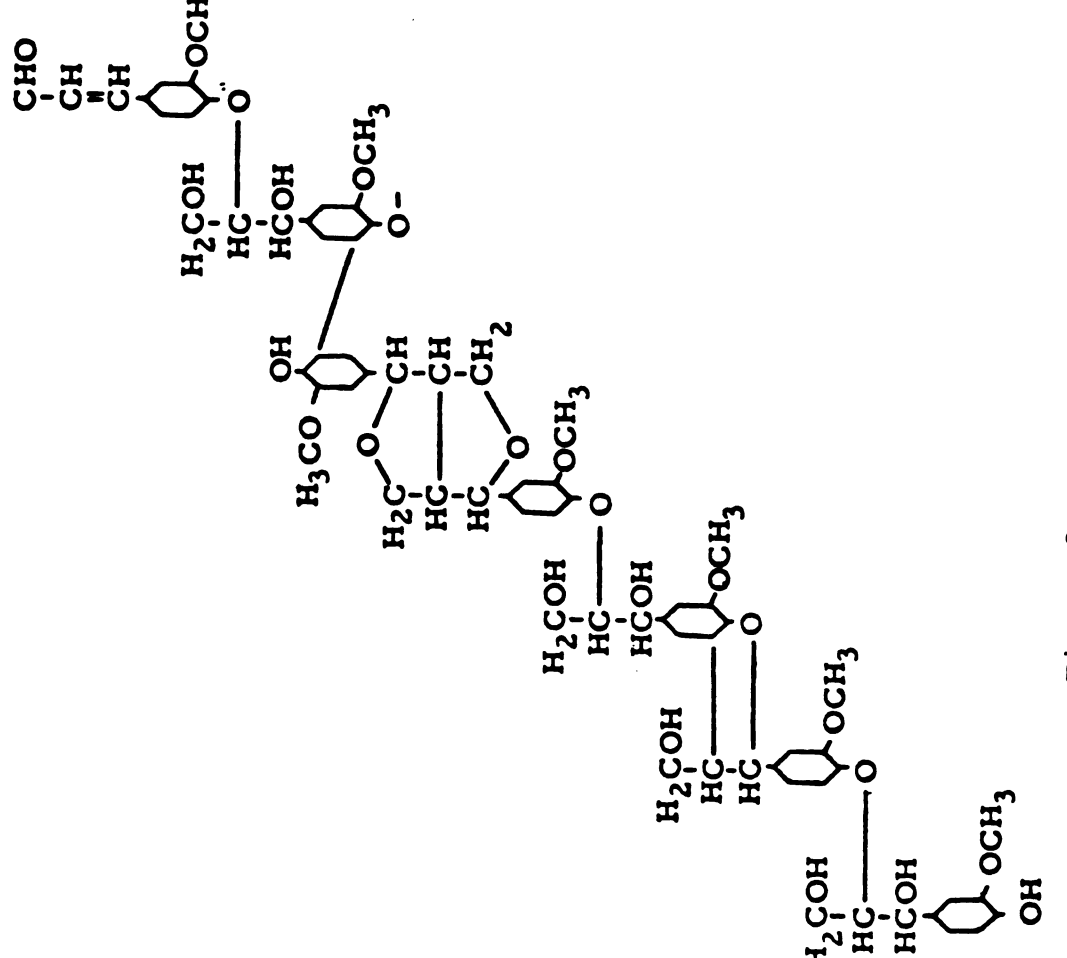


Figure 2. -- Chemical Structure of Lignin.

The structure of wood is primarily composed of cells called fibers or tracheids. Figures 3a and 3b are microphotographs of Poplar SPP showing a cross sectional view and a transverse view. Poplar fibers have an average length of 1.3 mm and diameter of 20 microns (2). Pits are small openings in the cell walls that allow for transport of material between cells. Each fiber has from 50 to 300 pits (1).

The cell wall is a multilayered structure with an intercellular substance known as the middle lamella binding the cells together. The cells have a primary wall and a secondary wall. These walls are made of small cellulosic fibers called microfibrils which have a width of 8 to 30 nm (3). The microfibrils are embedded in a matrix of lignin and hemicellulose. The primary wall is an amorphous structure of microbibrils whereas the secondary wall is more structured. The middle lamella is composed of lignin.

Wood can be decomposed by thermal degradation at high temperatures, which is called pyrolysis, or by chemical reaction with steam at high temperatures, which is called gasification. Pyrolysis is accomplished by heating wood in an inert atmosphere such as nitrogen.

Browne (4) has classified pyrolysis as having four temperature zones, each of which spans a different

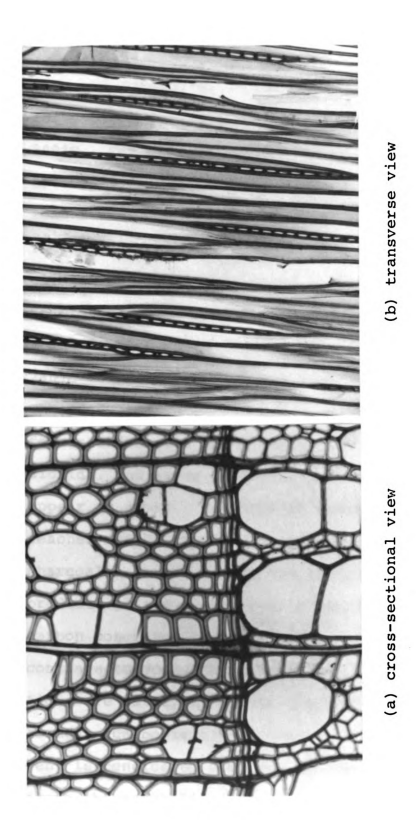


Figure 3. -- Microphotograph of Poplar SPP at 200 magnification.

temperature range. More than one zone may be present at one time as pyrolyzing wood has a temperature gradient from the outside to the center depending on the size of the particles. Zone A is defined for temperatures up to 200°C. The surface becomes dehydrated and the products are water, carbon dioxide, and formic and acetic acids. Zone B includes reactions, which occur from 200°C to 280°C. The products are the same as from Zone A but in addition glyoxal and small amounts of carbon monoxide are formed. Endothermic decomposition reactions occur in both Zones A and B. Zone C is defined as the temperature range 280°C to 500°C in which the reactions become exothermic. The products are carbon monoxide, methane, formaldehyde, formic and acetic acids, methanol, hydrogen, carbon dioxide, and water. Droplets of highly inflammable tars appear as smoke. The smoking ceases by the time the wood reaches 400°C. The solid residue of pyrolysis is called charcoal. In many cases the primary liquid and gaseous products listed above undergo secondary reactions to form carbon monoxide, carbon dioxide, and hydrogen as they continue to contact the particle. The secondary reactions are catalyzed by the charcoal and ash that are formed. Carbonization, removal of most oxygen and hydrogen, is considered complete at 400°C. Above this temperature the crystalline structure of graphite is developed.

The original porous structure of the wood remains intact through carbonization. Zone D occurs where the temperature is above 500°C and the products are small amounts of carbon monoxide, carbon dioxide, and hydrogen. Since the wood may have more than one temperature zone present at a time the products in the interior, lower temperature zone, pass through the outer zones and undergo secondary reactions. Carbon dioxide and water react with the remaining carbon in Zone D to produce carbon monoxide and hydrogen.

Pyrolysis of the different components of wood occurs at different temperatures (4). Hemicellulose is pyrolyzed from 200°C to 260°C (Equation 1).

acetic acid
formaldehyde
carbon monoxide
hemicellulose → hydrogen
furfural
furan
char
(1)

It evolves mainly gas and few tars. Much of the acetic acid comes from hemicellulose. Cellulose pyrolyzes from 240°C to 350°C (Equation 2).

water
carbon dioxide
carbon monoxide
acetic acid
formic acid

cellulose + methane (2)
ethane
ethylene
hydrogen
levoglucosan
formaldehyde
char

First water is given off and then levoglucosan. Levoglucosan is stable up to 270°C and then undergoes reactions to form formic and acetic acids and formaldehyde. The pyrolysis of lignin occurs from 280°C to 500°C and yields more char than the pyrolysis of cellulose (Equation 3).

vanillin
syringaldehyde
guaiacol
catechol
cresol
phenol
lignin → xylenol
carbon dioxide
methane
ethane
ethylene
formic acid
acetic acid
methanol

Due to the aromatic structure of lignin many of the products are aromatic.

The pyrolysis products depend upon the rate of heating. Slow pyrolysis increases the charcoal formed

and decreases the tars formed. Rapid pyrolysis gives the opposite trends. Slow heating allows for an orderly decomposition of the material to occur. The products of the interior zones pass through the outer zones. heating is slow the products will pass through the outer zones slowly and there is time for secondary reactions to occur. The extent of the secondary reactions depends on how slow the heating rate is and thus the time that it takes for the primary products to pass through the outer zones. There is a stepwise formation of more stable compounds that are rich in carbon leading to a higher percentage of char. In rapid heating the decomposition is more violent resulting in volatile fragments which appear as tar. More tars are produced than in slow heating because the tars pass rapidly through the outer zones and the time for secondary reactions to take place is small. In the early stages of pyrolysis the gases are rich in hydrogen and oxygen. The carbonaceous residue assumes a hexagonal graphitic structure. The carboncarbon bonds are unbreakable by pyrolysis alone up to temperatures of 3000°C. Even after active pyrolysis ceases the remaining char contains hydrogen and oxygen. Upon heating to higher temperatures small amounts of hydrogen and carbon monoxide are given off. The char produced by pyrolysis is primarily carbon. Table 1 gives an elemental analysis of char that was produced from coconut at 950°C (5).

Table 1.--Elemental analysis of coconut char produced in nitrogen at 950°C.

|          | Weight % |
|----------|----------|
| Carbon   | 97.560   |
| Hydrogen | 0.440    |
| Oxygen   | 1.670    |
| Nitrogen | 0.190    |
| Ash      | 0.130    |
| Iron     | 0.001    |
| Halides  | 0.001    |
|          |          |

The following reactions, Equations 4 through 7, are considered important when considering gasification (6).

$$C + H_2O = CO + H_2$$
 (4)

$$co + H_2 o = co_2 + H_2$$
 (5)

$$C + 2H_2 = CH_4$$
 (6)

$$2co = co_2 + c \tag{7}$$

Gasification occurs when steam is reacted with the char and produces hydrogen and carbon monoxide (Equation 4). The product gases can undergo further reactions; either with the steam or the original carbon. The water gas shift reaction, Equation 5, is often considered rapid and limited by equilibrium. Methane is formed by the reaction of hydrogen with carbon (Equation 6). Another possible reaction is the Boudouard reaction (Equation 7).

The rate expression for the gasification of coconut char has been determined by Blackwood and McGrory (5) to be Equation 8.

rate = 
$$\frac{k_1 p_{H_2O}}{1 + k_2 p_{H_2} + k_3 p_{H_2O}} \frac{mol}{min g}$$
 (8)

They used purified coconut char that was produced at 950°C in nitrogen. Each experiment used 8.8 g of B. S. sieve size -7 to +14 char in a differential reactor. Experiments were run at 750°, 790°, and 830°C with the partial pressures of steam and hydrogen varying from 0 to 50 atm and 0 to 3 atm respectively. The values of  $k_1$ ,  $k_2$ , and  $k_3$  at 830°C were found to be 3.7 x 10<sup>4</sup> mol/g min atm, 35 atm<sup>-1</sup>, and 0.14 atm<sup>-1</sup> respectively. The reaction rate was independent of space velocity indicating that the reaction was not controlled by external mass transfer

limitations. It was found that there was no significant change in the reaction rate up to conversions of 20% and the rate decreased by only 5% at 50% conversion. Hydrogen was an inhibitor of the reaction due to its strong adsorption to the active sites. As the hydrogen partial pressure increased the rate was lowered and as much as one-third of the carbon reacted to form methane. speculated that the active sites are carbon atoms to which oxygen atoms are already attached (5). When chars are prepared some oxygen is left in the structure. This would then form carbon monoxide at the start of the reaction and the steam would supply oxygen to the active sites when the original oxygen was removed. Hydrogen inhibition would occur when free hydrogen instead of oxygen from the steam was adsorbed. Steam attacking carbon in the above mechanisms would preserve the original bulk volume.

In systems involving carbon monoxide and steam the water gas shift reaction, Equation 5, is important. The reaction rate has been studied and rates determined by Graven and Long (7). They used a quartz reactor and found that quartz is not a catalyst of the reaction. However, in systems involving char, the ash is a catalyst. Blackwood and McGrory (5) found that varying the ash content has an effect on the carbon dioxide concentration

but not the steam-carbon reaction rate. When a char with an ash content of 0.26% was used, the product gases contained 20% carbon dioxide. When the ash content was decreased to 0.13%, the carbon dioxide concentration fell to 0.8%. Therefore the shift reaction is a function of the ash content and goes to equilibrium for high ash content coals and biomass. The shift reaction is undesirable if a product gas with a high heating value is wanted. It reduces the heating value by producing hydrogen and carbon dioxide which have a lower heating value than carbon monoxide.

Methane is also a product in steam-carbon systems. It is produced by the reaction of hydrogen, a product of steam gasification, and carbon. Blackwood (8) has determined the rate to be predicted by Equation 9.

rate = 
$$\frac{k_1 (p_H)^2 - k_2 p_{CH_4}}{1 + k_3 p_{H_2} + k_4 (p_H)^2 + k_5 p_{CH_4}} \frac{\text{mol}}{\text{g min}}$$
(9)

The apparatus and char samples were the same as for the gasification studies of Blackwood and McGrory (5). The temperature was varied from 650°C to 870°C and the hydrogen and methane partial pressures were varied from 0 to 40 atm and 0 to 20 atm respectively. The methane formation rate was determined to be independent of space

velocity. Unlike the gasification reaction, hydrogen is not an inhibitor of methane formation. The rate is linear with respect to the partial pressure of hydrogen at low partial pressures. It is postulated that the formation of methane is due to the formation of -CH2-CH2groups on the carbon surface. The rate controlling step is the breaking of the carbon-carbon bond. Methane is not formed until the adsorption of hydrogen is complete. The reactivity of chars for the formation of methane is dependent upon the temperature history of the char and is independent of the source of char in the case of different coals (9). The activation energy is the same for the different chars so the sites are assumed to be the same (10). The rate is different due to the quantity of active sites. Using a reaction temperature above that at which the char was produced causes a rapid deactivation.

The Bouduoard reaction also decreases the heating value of the product gas. The rate is slow in the gas phase and does not have a significant effect on the product gas composition (6).

The kinetics of coal char gasification have been studied for use in the design of in situ gasification. Fischer et al. (11) have determined the rate to be predicted by Equation 10.

rate = A 
$$(X_c)$$
  $(p_{H_2O})^m \exp(-E_a/RT)$   $\frac{g \text{ gasified}}{hr \text{ g remaining}}$  (10)

They found that the value of m varies with conversion of coal, X. For the first 20% of conversion m appears to be 1.3 and then decreases to 1.2 for higher conversions. The manner in which the char was prepared was found to have an effect on the reactivity. Two different chars were used; one formed in the gasification reactor directly before the gasification started and one formed in another reactor. Both chars were made from Wyodak coal but the conditions were different. The first was produced in argon at a heating rate of 3°C/min and the final temperature was 700°C. The second was produced at the same heating rate but with a maximum temperature of 800°C. Also the latter was exposed to the air when it was transferred from the reactor it was prepared in to the reactor it was gasified in. The latter char was found to have a rapid decrease in reactivity during the gasification The reaction was found to be diffusion experiments. limited at temperatures above 700°C due to the small pore structure of coal char. The ratio of hydrogen to carbon dioxide was found to be approximately 2:1. This is due to the water gas shift reaction approaching equilibrium.

Coal char gasification has also been studied by Taylor and Bowen (12). Their results are similar to the

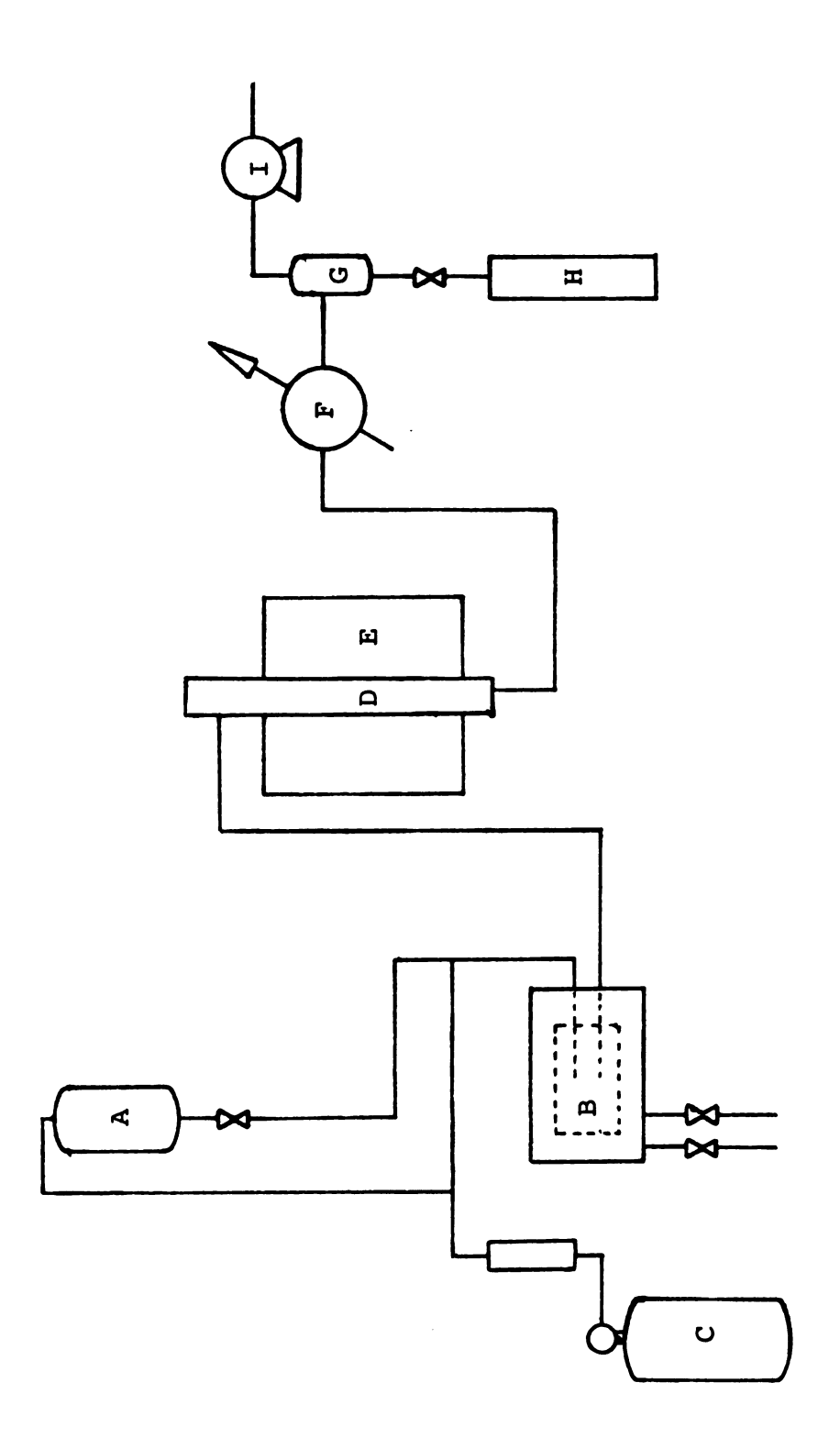
results described above. It was found that the rate was proportional to the char remaining. The rate was the same for different space velocities indicating reaction control in the temperature range studied (< 700°C). A maximum rate was found to occur at 30% to 40% conversion of the char. Chars made at 800°C were ten times less reactive than chars made at 600°C. This decrease in reactivity was also observed by Blackwood et al. (10) in their study on methane formation from different coal chars. It was speculated that the structure was condensed more at higher temperatures thus reducing the number of the active sites.

### EXPERIMENTAL APPARATUS AND PROCEDURES

## Apparatus

The gasification of wood is studied using a differential reactor. The reaction occurs by reacting steam with the char to produce a product gas consisting of carbon monoxide, carbon dioxide, methane, and hydrogen.

A diagram and photographs of the experimental apparatus are shown in Figures 4, 5, and 6. Steam for the reaction is produced by feeding water gravimetrically from a three liter bottle to a gas furnace. gas furnace consists of a steel shell with a ceramic inner shell. Asbestos is used as an insulating material between the shells. The steam is vaporized in a stainless steel cylinder which measures 13 cm long and has a diameter of 3.9 cm. The flame in the furnace is adjusted with valves controlling the air flow and the gas flow. The flow rate of steam is regulated by controlling the water flow with a needle valve. Nitrogen is supplied from a regulated cylinder and serves two purposes. creates a pressure differential which causes the steam to flow and is used as an inert to vary the steam partial



paratus: (A) water bottle, (B) (D) reactor, (E) electric furnace, (H) 250 ml graduated cylinder, Figure 4.--Schematic diagram of gasification apparatus:
gas furnace, (C) nitrogen cylinder, (D) reacto
(F) condenser, (G) 50 ml separator, (H) 250 ml
and (I) wet test meter.

|  |  | •                                     |
|--|--|---------------------------------------|
|  |  |                                       |
|  |  | •                                     |
|  |  |                                       |
|  |  |                                       |
|  |  | 1                                     |
|  |  |                                       |
|  |  |                                       |
|  |  |                                       |
|  |  | į                                     |
|  |  |                                       |
|  |  |                                       |
|  |  |                                       |
|  |  |                                       |
|  |  |                                       |
|  |  | · · · · · · · · · · · · · · · · · · · |
|  |  |                                       |
|  |  |                                       |
|  |  |                                       |
|  |  |                                       |
|  |  |                                       |
|  |  |                                       |
|  |  |                                       |
|  |  |                                       |
|  |  |                                       |

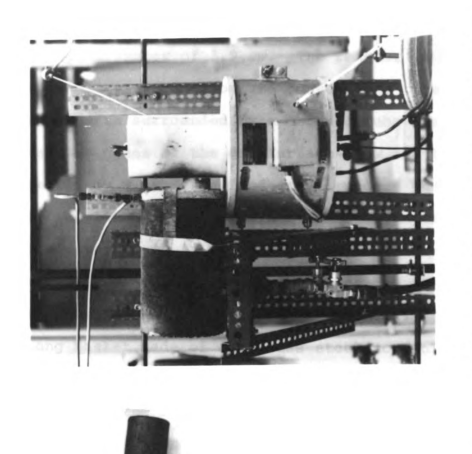


Figure 5.--Photograph of gasification Figure reactor.

Figure 6.--Photograph of gasification apparatus.

The superheated steam flows to a stainless pressure. steel reactor (Figure 5) that is 34.3 cm long and has an inside diameter of 3.9 cm. The reactor is heated by two mechanisms; conduction and convection. The top of the reactor is surrounded by a ceramic tube through which the exhaust gases of the gas furnace flow and the bottom is heated by a one zone Lindberg furnace, The electric furnace is controlled with a Wheelco temperature controller. The temperature is monitored using chromel-alumel thermocouples; one at the steam inlet and one at the bottom of the sample basket. The sample is contained in an 8 cm long basket made of stainless steel screen. The top of the reactor is a removable cap and the sample is manually placed in the reactor when the reaction temperature is attained. After the reactor the steam is condensed in a copper coil using tap water as a condensing fluid. At the outlet of the condenser is a 50 ml cylinder which is connected to a 250 ml graduated cylinder. A valve between the two allows for a constant level in the small cylinder. The small cylinder is used to separate the product gases from the water and its small size minimizes mixing of the gases. The gases then pass through a Drierite column to remove any entrained water before gas samples are taken. Samples are taken through a septum using 2 ml gas syringes. The gas then passes through a wet test meter which measured total gas flow.

## Sample Preparation

The species of wood used for this study was

Poplar SPP. A hammer mill was used to grind the wood

into particles approximately 5 mm long and 1 to 2 mm in

thickness and width. The wood was sifted to remove very

fine particles, the sawdust. The particles, 5 mm long

and 1 to 2 mm thick, were then dried overnight at 100°C

to remove moisture. The initial weight was reduced an

average of 48% by drying. In order to produce char for

the gasification experiments the dried wood was pyrolyzed.

The char used in the experiments was pyrolyzed at 700°C for 10 minutes. Nitrogen was used as the inert atmosphere and the flow rate was set at 2 1/min at STP. After the sample was removed from the reactor it was flushed in nitrogen to prevent combustion of the remaining char. The wood had a weight loss of 86% during this process. The char was stored in a desiccator to prevent adsorption of water.

A temperature of 700°C was chosen so that gasification experiments would not be run at temperatures higher than the temperature at which the char was made. If the experimental gasification temperature was higher than the pyrolysis temperature a rapid deactivation in the gasification rate would be expected (10). A temperature higher than 700°C was not used for pyrolysis because

the reactivity decreases as the pyrolysis temperature increases. The pyrolysis time was varied to determine the weight loss versus pyrolysis time. Figure 7 shows that most of the weight loss occurs during the first minute. The weight loss during that minute was 81% of the original weight and after eight minutes 86% of the original weight had been lost.

taken through an electron microscope it can be seen that the original cell structure remains intact even after pyrolysis. The char in the photographs was produced in a gasification environment. The temperature was 600°C and the steam partial pressure was 100 kPa. Even though a gasification environment was used pyrolysis was the main reaction occurring. The cell walls appear thinner and the surface is much smoother after pyrolysis. There appears to be no structural differences between the sample pyrolyzed for one minute and the sample pyrolyzed for eight minutes.

## Operating Procedure

Before the experiments were run, a steady state temperature was obtained in the gasification apparatus (Figure 4). The process was started by igniting the gas furnace and turning on the electric furnace. After the

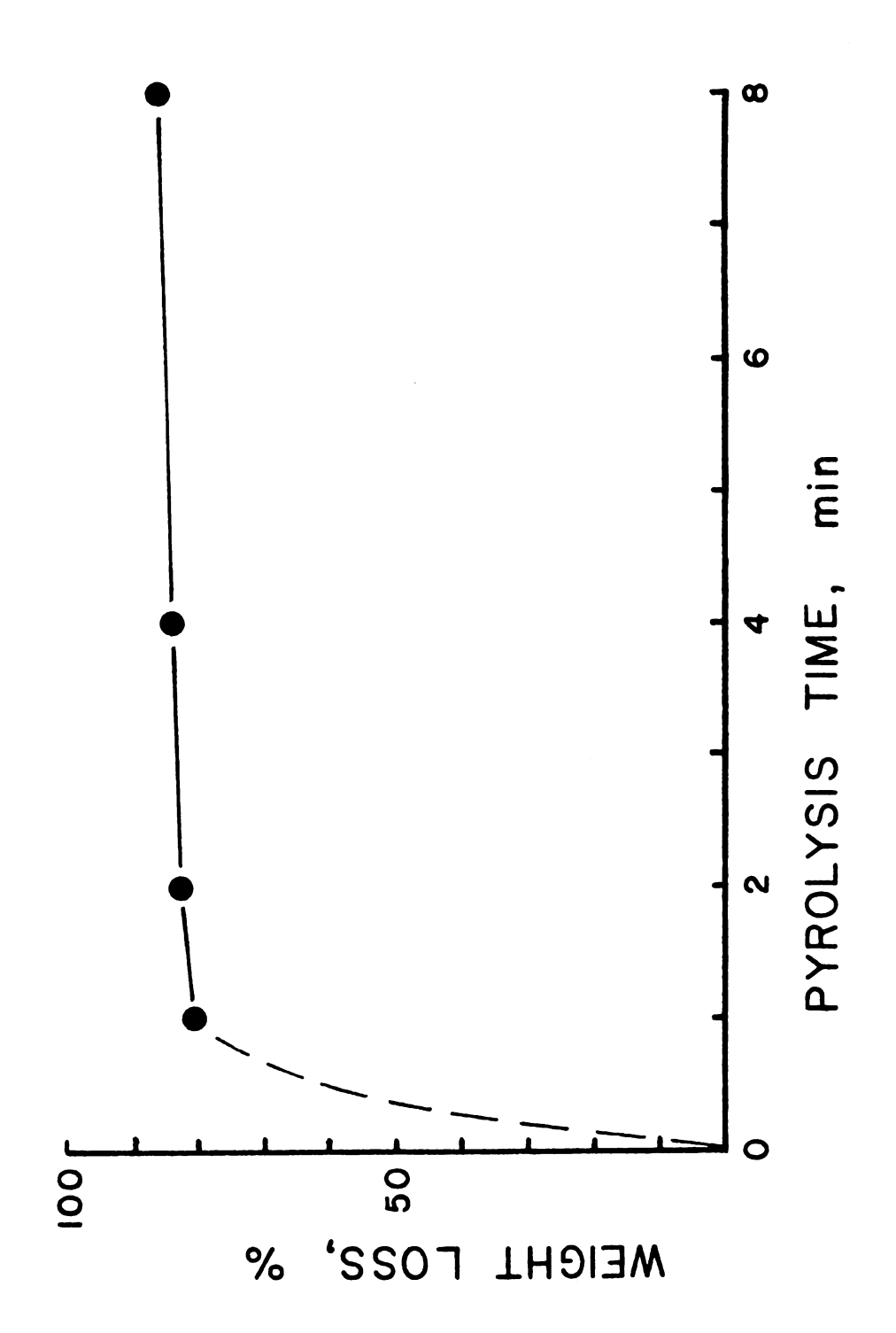
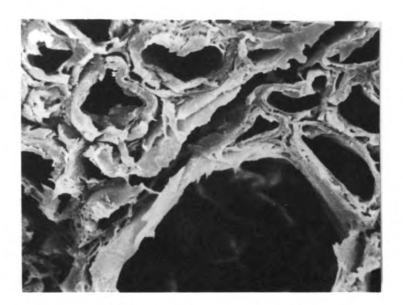
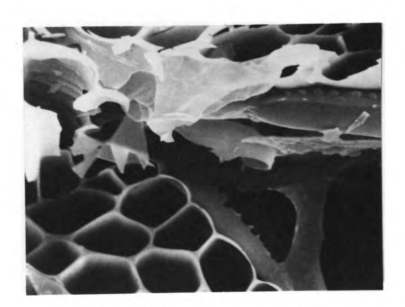


Figure 7.--Pyrolysis weight loss versus pyrolysis time for Poplar SPP in nitrogen at 700°C.

26



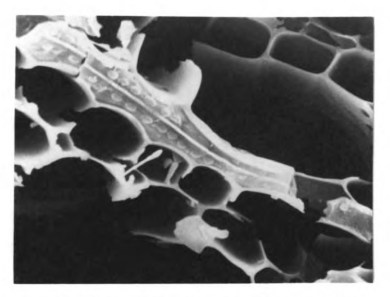
(a) before pyrolysis



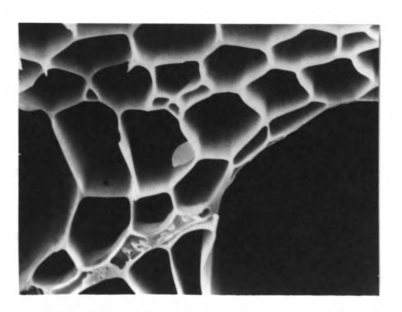
(b) after 1 minute of pyrolysis

Figure 8.--Microphotograph of Poplar SPP before and after pyrolysis at 600°C and steam partial pressure of 80 kPa.

27



(c) after 4 minutes of pyrolysis



(d) after 8 minutes of pyrolysis

Figure 8. (continued)

gas furnace had heated to over 100°C the nitrogen and water flow were begun. Initially, the nitrogen flow was high and the water flow was low. This prevented a buildup in pressure that would back up water into the nitrogen flow meter. After steam condensate was seen at the outlet of the condenser the nitrogen and water flow rates were adjusted to the desired levels. These levels were determined by the partial pressure and space velocity The water flow rate was determined by measuring the condensate collected over a known period of time, usually five minutes. The nitrogen flow was determined using the wet test meter. When the reaction temperature was reached the controls on the gas furnace were adjusted to give a constant temperature. The nitrogen and water flow rates were again measured and adjustments were made if necessary. The bottom temperature was set slightly higher than the reaction temperature to compensate for a drop in temperature that occurred when the sample was placed in the reactor. This pre-experiment process required between one and two hours.

To begin the experiment the top of the reactor was removed and the basket containing the samples was placed in the reactor. The basket had a volume of 92 cm<sup>2</sup> and contained 2.6 to 2.7 g. The timer was started and the initial water levels in the separators were recorded.

Gas flow readings on the wet test meter and both temperatures were recorded every minute. The controller on the electric furnace was operated manually. Gas samples were taken with gas syringes at various intervals depending on the reaction conditions. The low temperature experiments were run longer than the high temperature experiments. The experiments were ended when the gas production started to decline. The sample was removed and weighed and final readings were taken on the wet test meter and water levels.

# Gas Analysis

The gas samples were analyzed using gas chromatography. Using this technique, the relative amounts of hydrogen, nitrogen, carbon monoxide, methane, and carbon dioxide in the product gas were determined. The gas chromatograph used was a Perkin-Elmer Model 154 which utilized a thermal conductivity detector. Carbosieve S packing was used in a column 1830 mm long with an inside diameter of 3.174 mm. Neon was used as the carrier gas in order to measure hydrogen (11). Originally helium was tried as a carrier gas but hydrogen could not be detected although the other gases could. A strip chart recorder was used to record the output.

The chromatograph was calibrated by injecting a measured quantity  $(0.5 \text{ cm}^3)$  of each of the pure gases.

The Appendix gives the details of the calibration. It was assumed that the relationship of quantity versus peak area was linear for all of the gases.

The data were analyzed by determining the relative amounts of each gas present in the sample. The area under the peaks of the gas chromatograph output was determined by cutting out and weighing the peak. The relative amount was calculated using Equation 11 where  $\mathbf{w}_i$  is the weight of the peak and  $\mathbf{f}_i$  is the calibration factor.

mole fraction of component 
$$i = \frac{f_i w_i}{n}$$
 (11)
$$\sum_{i=1}^{\Sigma} f_i w_i$$

### RESULTS

Experiments were conducted to determine the gasification rate of Poplar SPP char for various space velocities (2.0 s<sup>-1</sup> to 7.3 s<sup>-1</sup>), steam partial pressures (46 kPa to 100 kPa), and temperatures (550°C to 685°C). Between 2.6 and 2.7 grams of ground wood char was used in each gasification experiment. Three different space velocities at a constant steam partial pressure (100 kPa) and constant temperature (625°C) were studied. Four different steam partial pressures at a constant space velocity (4 s<sup>-1</sup>) and temperature (625°C) and three temperatures at a constant space velocity (4 s<sup>-1</sup>) and constant steam partial pressure (11 kPa) were also studied. A summary of experimental conditions and results is contained in Tables 2, 3, and 4.

The first series of experiments was run to determine the effect of space velocity on the gasification rate. Three experiments were conducted at a constant temperature of 625°C and a constant steam partial pressure of 100 kPa for three values of space velocity; 2.0 s<sup>-1</sup>, 3.6 s<sup>-1</sup>, and 7.3 s<sup>-1</sup>. Results of the space velocity experiments are shown in Figure 9. The rate of gasification

TABLE 2.--Summary of gasification rate results for varying space velocities at 625°C and steam partial pressure of 100 kPa.

|         | Error                                                              | 21.6  | -2.1  | -12.5 |
|---------|--------------------------------------------------------------------|-------|-------|-------|
| Case II | Calculated<br>Rate x 10 <sup>3</sup><br>mol/g min                  | 3.547 | 3.542 | 3.554 |
|         | Measured<br>Rate x 103<br>mol/g min                                | 4.314 | 3.467 | 3.109 |
|         | Error<br>%                                                         | -8.4  | 9.6-  | -39.5 |
| Case I  | Calculated<br>Rate x 103<br>mol/g min                              | 3.748 | 3.737 | 3.767 |
|         | Space Measured<br>Velocity Rate x 10 <sup>3</sup><br>s-l mol/g min | 3.433 | 3.377 | 2.278 |
|         | Space<br>Velocity<br>s-1                                           | 2.0   | 3.6   | 7.3   |

TABLE 3.--Summary of gasification rate results for varying steam partial pressures

|                           |         | Error<br>8                                      | 1.3   | -3.0  | 4.1   | -2.1  |  |
|---------------------------|---------|-------------------------------------------------|-------|-------|-------|-------|--|
|                           | Case II | Calculated<br>Rate x 103<br>mol/g min           | 2.364 | 2.834 | 3.358 | 3.542 |  |
|                           |         | Measured<br>Rate x 10 <sup>3</sup><br>mol/g min | 2.395 | 2.749 | 3.496 | 3.467 |  |
| d space velocity of 4 s-1 |         | Error<br>8                                      | 14.1  | -10.4 | 5.4   | 9.6-  |  |
| d space veloc             | Case I  | Calculated<br>Rate x 103<br>mol/g min           | 1.736 | 2.369 | 3.316 | 3.737 |  |
| at 625°C and              |         | Measured<br>Rate x 10 <sup>3</sup><br>mol/g min | 1.981 | 2.122 | 3.496 | 3.377 |  |
|                           |         | Partial<br>Pressure<br>kPa                      | 46.41 | 63.33 | 88.66 | 99.91 |  |

TABLE 4.--Summary of gasification rate results for varying temperature at steam

| Temperature<br>°C | Measured<br>Rate x 103<br>mol/g min | Calculated Rate x 10 <sup>3</sup> mol/g min | Error<br>8 | Case II  Measured Rate x 103 mol/g min |
|-------------------|-------------------------------------|---------------------------------------------|------------|----------------------------------------|
| 550               | .3652                               | .4127                                       | -9.3       | .5027                                  |
| 625               | 3.3770                              | 2.7660                                      | 22.1       | 3.4670                                 |
| 685               | 8.9020                              | 10.2140                                     | -12.8      | 8.9020                                 |

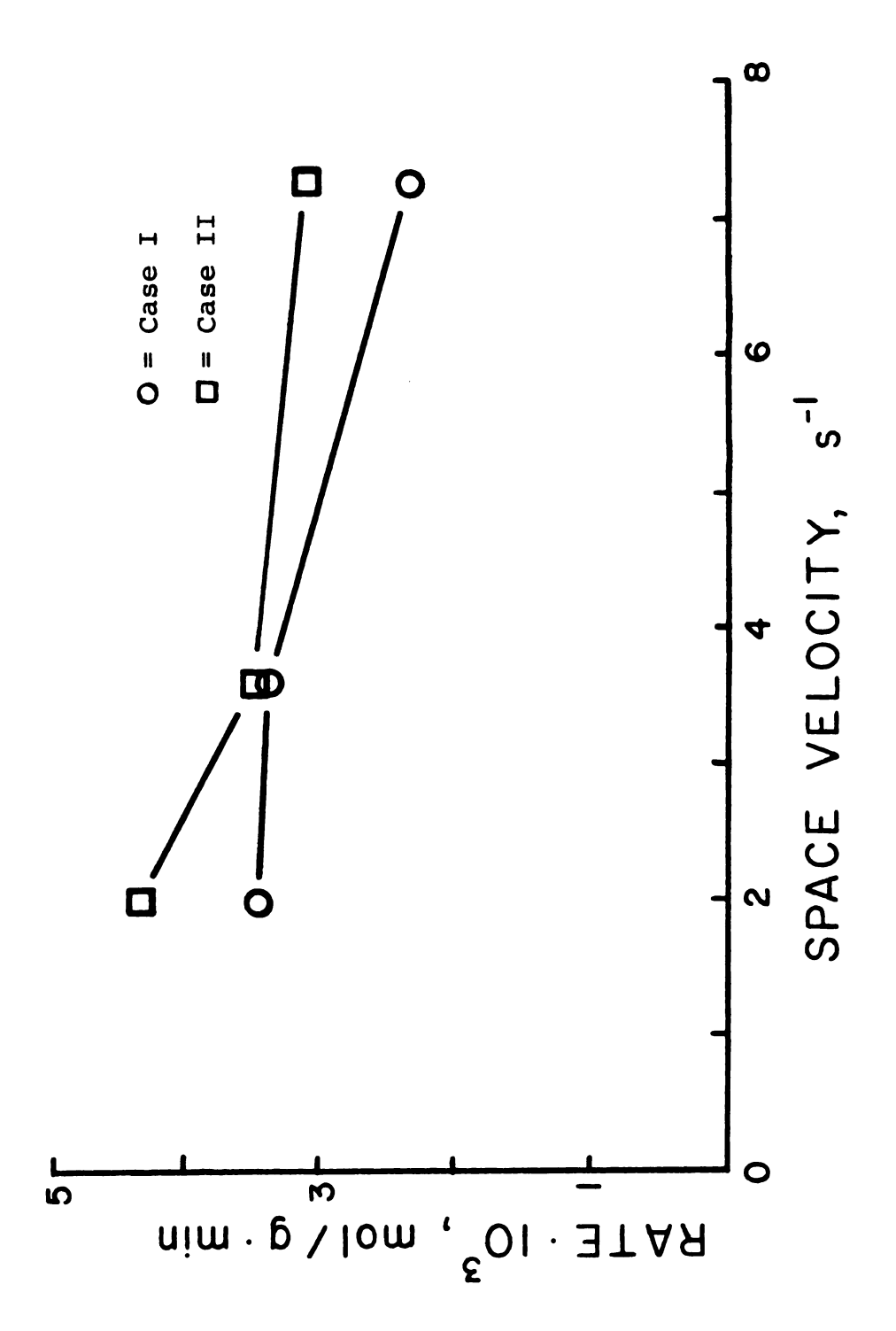


Figure 9.--Gasification rate of Poplar SPP char versus space velocity at 625°C and steam partial pressure of 100 kPa.

was calculated based on two different assumptions (see Appendix for sample calculations). In Case I, the rate of gasification was calculated based on the carbon in the carbon oxides of the product gas assuming a backmix reactor. In Case II, the rate of gasification was calculated based on the carbon contained in the carbon oxides and the methane in the product gas assuming a backmix reactor. Case I corresponds to assuming the methane was produced by direct hydrogenation of the char, while Case II corresponds to methane being produced by the reaction of carbon monoxide with hydrogen. The space velocity was defined as the volumetric gas flow rate at the inlet conditions divided by the volume of the sample basket  $(92 \text{ cm}^3)$ . As can be seen in Figure 9, the gasification rate in both cases decreased as the space velocity The decrease in rate was attributed to increased. experimental error in measuring the gas production or the reactor temperature and not a real effect of space velocity. Since the rate did not increase with an increasing space velocity it appeared that external mass transfer was not rate controlling. All further experiments were conducted at a space velocity of 4 s<sup>-1</sup>.

The effect of the steam partial pressure on the gasification rate was investigated in the next series of experiments. The steam partial pressure was varied from

46 kPa to 100 kPa while the total pressure and temperature were kept at 101 kPa and 625°C respectively. Nitrogen was used as an inert to obtain four values of steam partial pressure; 46, 63, 89, and 100 kPa. From Figure 10 it can be seen that the gasification rate was proportional to the steam partial pressure for Case I. For Case II (Figure 11) the gasification rate was less than first order with respect to steam.

The temperature was varied in a series of experiments to determine the activation energy of the reaction. Experiments were made at 550°C, 625°C, and 685°C at a steam partial pressure of 100 kPa and a space velocity of 4 s<sup>-1</sup>. From the graph of ln (rate) versus the reciprocal of the absolute temperature, Figure 12, the activation energy was calculated to be 156 kJ/mol for Case I. There was not enough data taken to determine the activation energies for Case II.

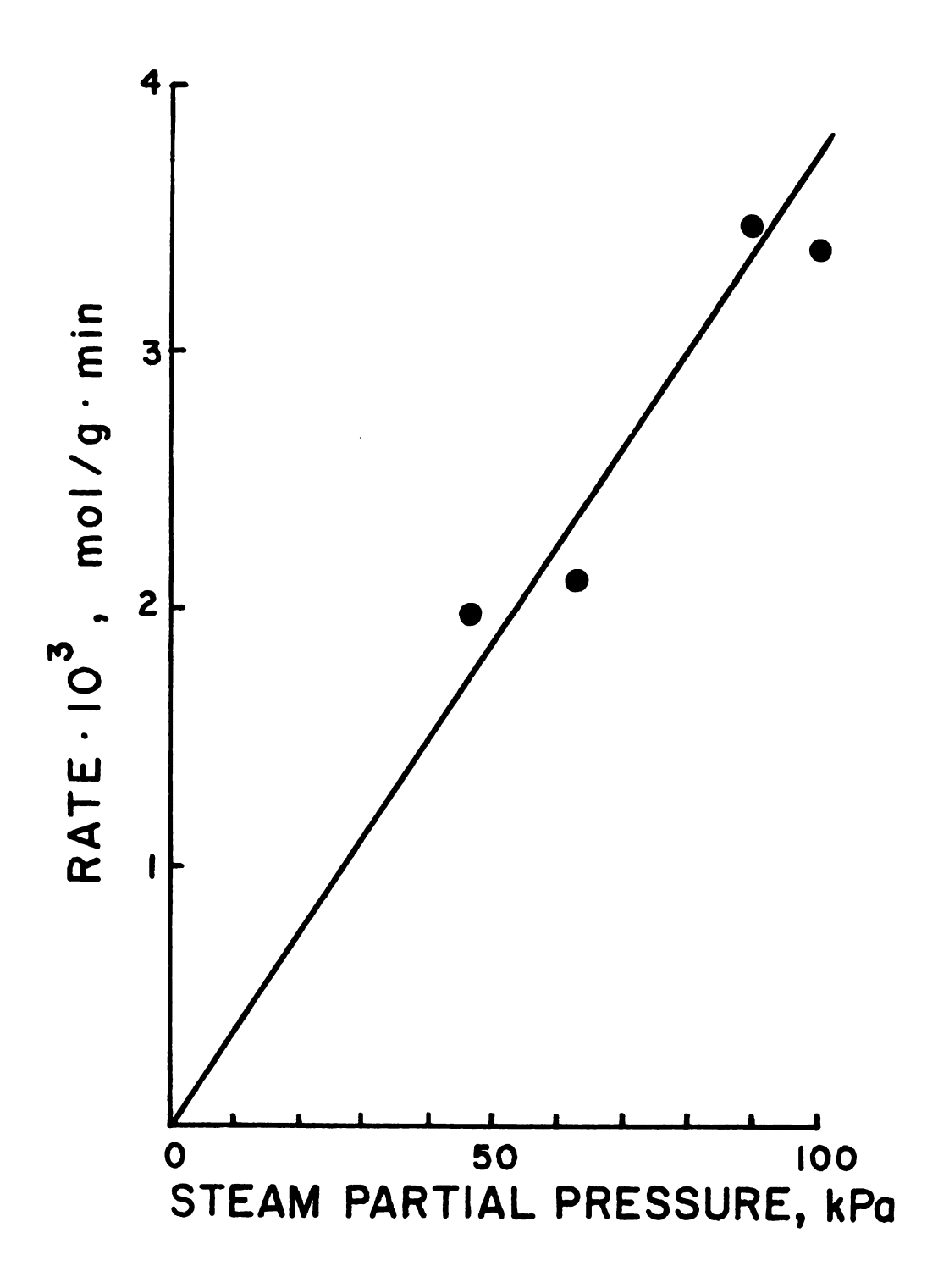


Figure 10.--Gasification rate of Poplar SPP char versus steam partial pressure at 625°C and space velocity of 4 s $^{-1}$  (Case I).

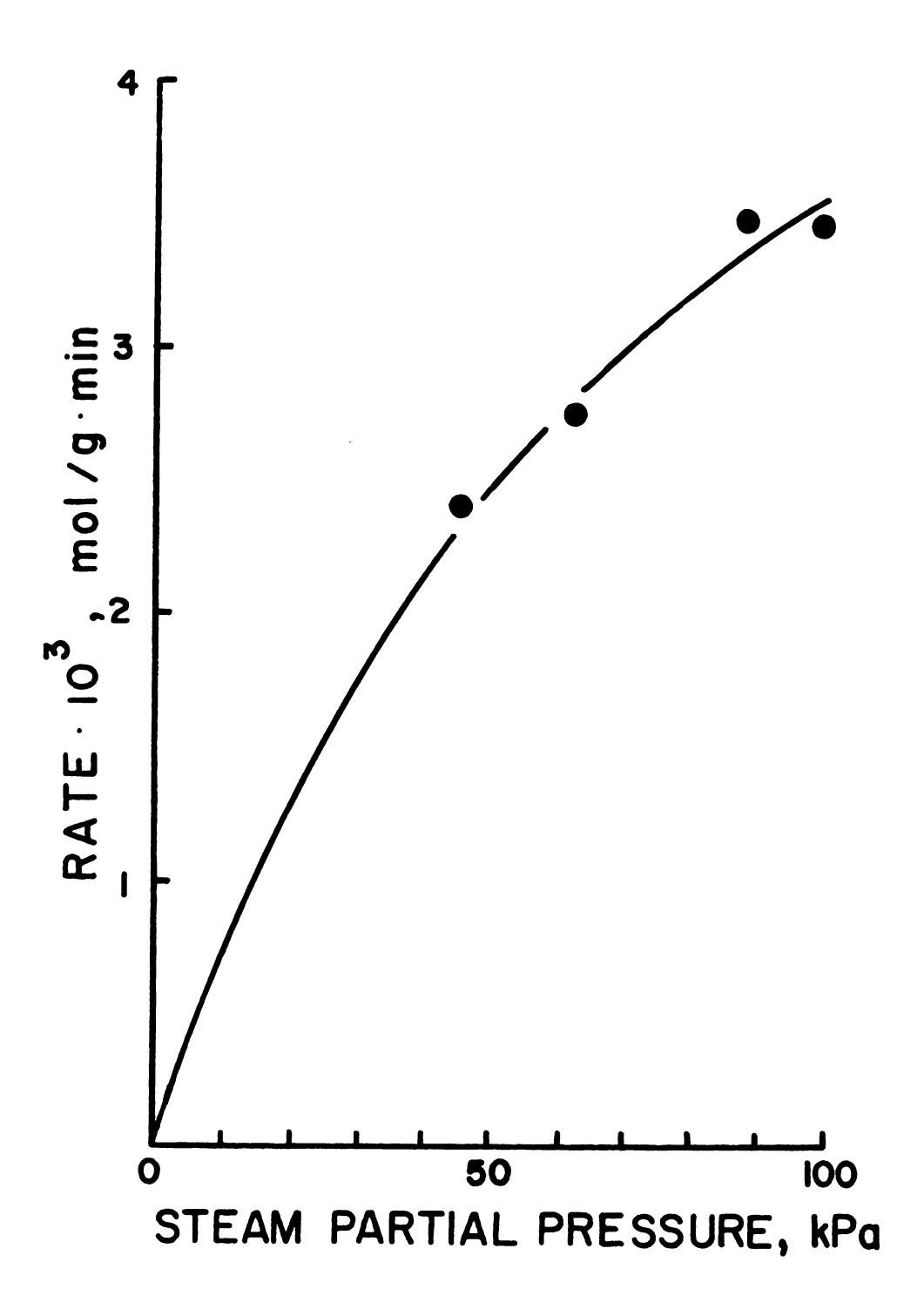


Figure 11.--Gasification rate of Poplar SPP char versus steam partial pressure at 625°C and space velocity of 4 s $^{-1}$  (Case II).

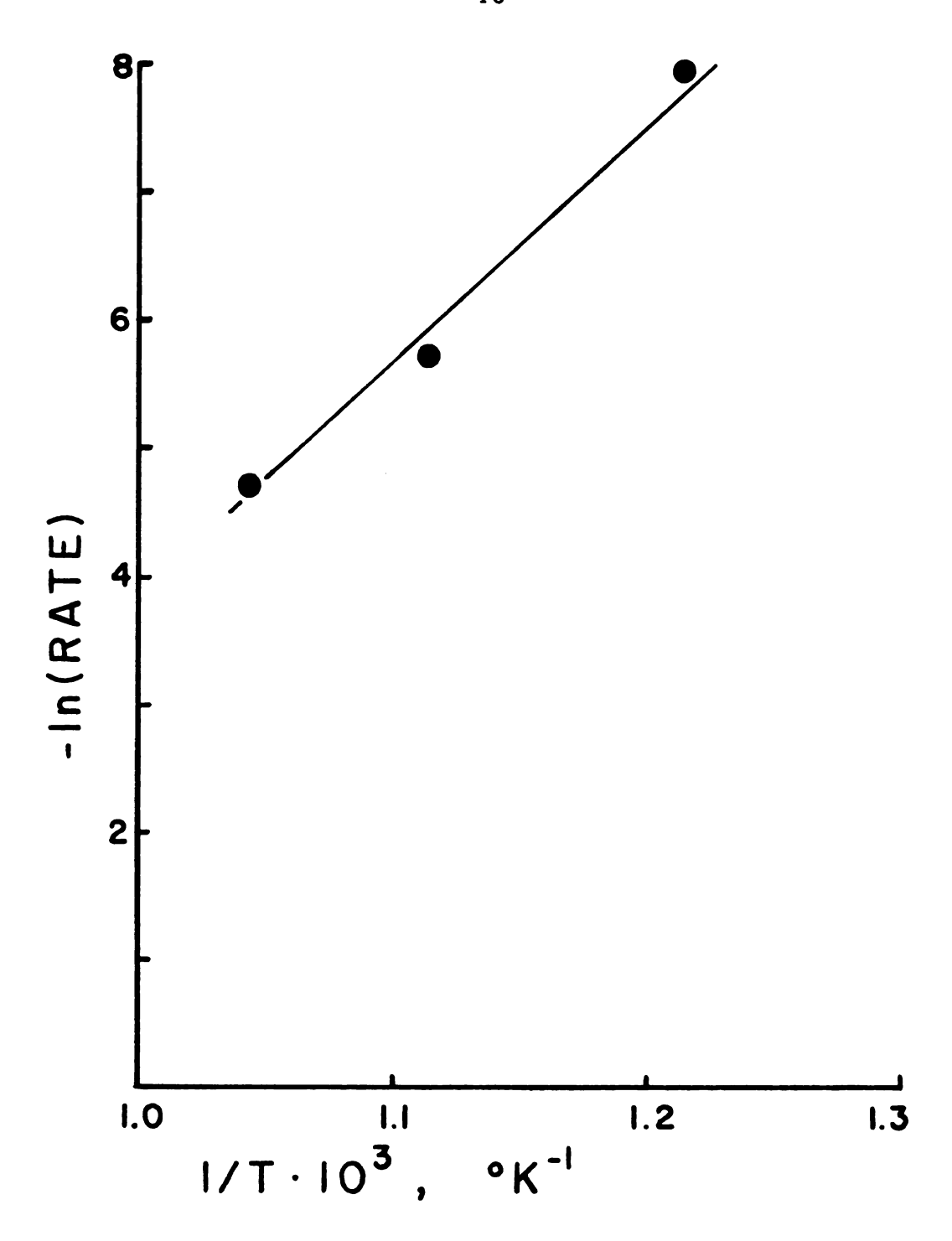


Figure 12.--Natural log of gasification rate (mol/g min) of Poplar SPP char versus inverse temperature at steam partial pressure of 100 kPa and space velocity of 4 s $^{-1}$ .

### DISCUSSION OF EXPERIMENTAL RESULTS

### Kinetics

The particles of char used in the experiments were small so it was assumed that there were no concentration gradients in the char. This assumption was verified based on calculations of effectiveness factors versus particle size. Since there was no external mass transfer resistance as determined experimentally and no diffusional resistance as determined from studies of effectiveness factor, the experimentally measured rate of gasification of the char represented the intrinsic kinetics. The rate of char consumed by gasification was calculated from the gaseous products in two different ways. The gases in the reactor were considered well mixed so the reactor was analyzed as a backmix reactor. The product gas, as determined on a nitrogen free basis, had a composition that was approximately 10% for both methane and carbon monoxide, 55% hydrogen, and 25% carbon dioxide. The rate of gasification can be calculated from the carbon in the carbon oxides only or from the carbon oxides plus the methane. It was not certain whether the methane was produced from the char or from the carbon

monoxide. It was speculated by other workers (5) that the methane was produced from the reaction of hydrogen or steam with -CH<sub>2</sub> groups on the carbon surface. Methane could also be produced from reaction of carbon monoxide and hydrogen in the product gas (Equation 12).

$$CO + 3H_2 = CH_4 + H_2O$$
 (12)

Both assumptions were considered in treating the data.

In Case I the rate of gasification was calculated from the carbon oxides only and in Case II the rate was calculated from the carbon oxides plus the methane.

# Case I - Gasification Rate Based on CO and CO<sub>2</sub>

Four experiments were made varying the steam partial pressure. From Figure 10, the gasification reaction appears to be first order with respect to the steam partial pressure. From the partial pressure experiments with the following rate expression was determined (Equation 13).

$$rate = k p_{H_2O} \frac{mol}{min g}$$
 (13)

The rate is expressed in gram moles of carbon gasified per minute per original gram of carbon present. The partial pressure of steam is expressed in kPa and k has

a value of  $3.74 \times 10^{-5}$  mol/min g kPa. Figure 10 shows the experimental points and the relationship predicted by Equation 13. In the experiments, the gasification rate was the highest for the steam partial pressure of 89 kPa. This cannot be explained as this experiment was run exactly as all of the other experiments.

The activation energy was found to be 156 kJ/mol from Figure 12. This is within the same order of magnitude as activation energies found for coal char gasification. Fischer et al. (11) studied chars made from two different coals. Between 640°C and 700°C, they found activation energies of 318 kJ/mol and 222 kJ/mol and at temperatures higher than 700°C they found that the values decreased to 63 and 113 kJ/mol respectively. This indicated that diffusion was quite likely controlling at temperatures greater than 700°C.

Comparison of activation energies for coal char and wood char gasification indicated that kinetics and not diffusion were controlling under the conditions of this study. The first order rate constant can be expressed by Equation 14.

$$k = k_0 \exp(-E_a/RT)$$
 (14)

From the variable temperature experiments  $k_0$  was found to be 32,860 mol/g min kPa.

# Case II - Gasification Rate Based on CO, CO<sub>2</sub>, and CH<sub>4</sub>

partial pressure experiments where the gasification rate was calculated from the carbon in the carbon oxides plus the methane. The curve in Figure 11 shows the rate versus the steam partial pressure as predicted by a Langmuir type rate expression (Equation 15).

rate = 
$$\frac{k_1 p_{H_2O}}{1 + k_2 p_{H_2O}} \frac{mol}{min g}$$
 (15)

The constants,  $k_1$  and  $k_2$ , were determined to be 8.203 x  $10^{-5}$  mon/min g kPa and 1.315 x  $10^{-2}$  kPa<sup>-1</sup> respectively at 625°C. The above expression is comparable to the expression derived from an adsorption-desorption mechanism (Equation 24) which is discussed later under Modeling. When the hydrogen partial pressure is low, as is the case in this study, the  $(k_3 \ P_{H_2O} \ P_{H_2})$  term can be neglected so the derived expression (Equation 24) is the same as Equation 15. There was insufficient data to determine the activation energies of  $k_1$  and  $k_2$ .

Figure 9 shows the results of the space velocity experiments with the gasification rate being calculated for both Case I and II. In the experiment where the space velocity was the highest  $(7.3 \text{ s}^{-1})$ , the gasification

rate was the lowest for that series of runs. This was attributed to experimental error in measuring the temperature or the gas flow rate and not a real effect of space velocity. If external mass transfer were controlling the reaction rate would increase with an increase in space velocity for any reaction of a positive order. A negative order reaction would have a decrease in reaction rate with increasing space velocity. The gasification reaction appears to be either first order (Figure 10) or Langmuirian (Figure 11) so the decrease in rate with increasing space velocity is a contradiction. For this reason the resulting lower gasification rate at a high space velocity was attributed to experimental error.

### Error Analysis

A mass balance was done to determine if the measured amount of char consumed by reaction equalled the amount calculated from the gas production. As an elemental analysis of our char was unavailable, it was assumed to be 100% carbon. This assumption was used since other workers (5) have found char to be over 97% carbon. The calculated amount was determined by multiplying the weight fraction of carbon in the product gases by the total gas produced (see Appendix for details). The error was less than 10% in all but three experiments and was less than 17% in those three. One possible source

of error was that char particles could be carried out of the sample basket by the flowing gases. These losses were minimal because the basket was made of a very fine screen. Another source of error is that the product gas compositions were an average of the gas samples taken. When the char was first placed in the reactor the gasification rate was low until the char reached the reaction temperature. Therefore the carbon composition of the product gas was actually lower than that used to calculate the char reacted which results in a higher calculated value than the measured value.

Tables 2, 3 and 4 give the measured rate, calculated rate, and the error for both Case I and Case II.

From Table 3 it can be seen that the error between the calculated rate and the measured rate was much less for Case II in the steam partial pressure experiments. The maximum error in Case II was 4.1% and was 14.1% in Case I. This is evidence that the methane was probably produced from the carbon monoxide and not directly from the char.

One possible source of error in all of the experiments was a temperature variation. The reaction temperature was controlled by manually operating the temperature controller to minimize temperature variations. At times the temperature would vary up to 5°C. Another source of

error would be the dissolving of some of the product gas in the condensing steam. This was assumed to be negligible. The product gas flow was measured using a wet test meter. At low steam partial pressures the nitrogen flow was high causing rapid movement on the needle on the wet test meter. Due to this rapid movement error could have been made in the readings. Since the flow was averaged over several minutes this error would be minimized. Averaging the product gas composition could introduce error. The composition of each gas sample was not exactly the same so they were averaged. This would create an error in determining the carbon composition in the product gas and thus the gasification rate.

# Equilibrium Considerations

A computer program was developed to calculate equilibrium constants and compositions for the steam-char system. It was based on a system where the reactions represented by Equations 4, 5, and 6 take place simultaneously. Figure 13 shows the equilibrium mole fractions of steam, carbon monoxide, carbon dioxide, hydrogen, and methane as a function of temperature. As the temperature increases the products go mainly to carbon monoxide and hydrogen. Low temperatures increase the relative amount of methane.

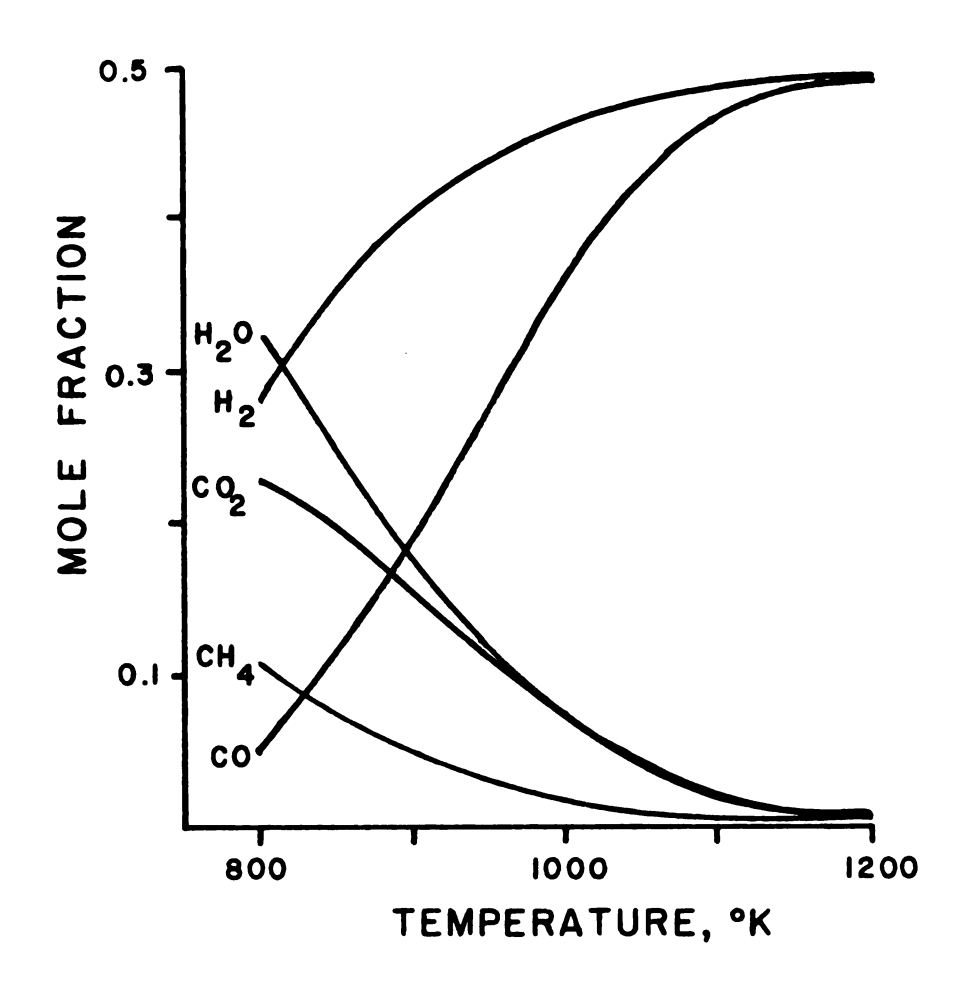


Figure 13.--Equilibrium mole fractions as a function of temperature for a steam-carbon system at a total pressure of 101 kPa.

It is common in coal gasification to consider the water shift reaction, Equation 5, to be in equilibrium.

This was not found to be true in the data taken in this study. Tables 5, 6, and 7 show that equilibrium was never reached due to the large amount of excess water.

In all experiments except one where methane was produced, the amount of methane produced was greater than was predicted by equilibrium for the reaction of hydrogen with carbon (Equation 6) at conditions in the reactor. This is not thermodynamically possible which indicates all of the methane was not produced from this reaction. It was possible that the methane was produced catalytically in the product gas stream by the reaction of carbon monoxide and hydrogen (Equation 12). This stream was at a temperature lower than the reaction temperature as it left the reactor outlet and passed through the condenser.

TABLE 5.——Average outlet gas compositions for the space velocity experiments at 625°C and steam partial pressure of 100 kPa.

| $\frac{{}^{y_{H_{2}}}{}^{y_{\infty_{2}}}{}^{y_{\infty_{2}}}{}^{k_{5}}{}^{y_{\infty_{4}}}{}^{k_{6}}{}^{x_{6}}{}^{x_{6}}{}^{x_{6}}{}^{x_{6}}{}^{x_{6}}{}^{x_{6}}{}^{x_{6}}{}^{x_{6}}{}^{x_{6}}{}^{x_{6}}{}^{x_{6}}{}^{x_{6}}{}^{x_{6}}{}^{x_{6}}{}^{x_{6}}{}^{x_{6}}{}^{x_{6}}{}^{x_{6}}{}^{x_{6}}{}^{x_{6}}{}^{x_{6}}{}^{x_{6}}{}^{x_{6}}{}^{x_{6}}{}^{x_{6}}{}^{x_{6}}{}^{x_{6}}{}^{x_{6}}{}^{x_{6}}{}^{x_{6}}{}^{x_{6}}{}^{x_{6}}{}^{x_{6}}{}^{x_{6}}{}^{x_{6}}{}^{x_{6}}{}^{x_{6}}{}^{x_{6}}{}^{x_{6}}{}^{x_{6}}{}^{x_{6}}{}^{x_{6}}{}^{x_{6}}{}^{x_{6}}{}^{x_{6}}{}^{x_{6}}{}^{x_{6}}{}^{x_{6}}{}^{x_{6}}{}^{x_{6}}{}^{x_{6}}{}^{x_{6}}{}^{x_{6}}{}^{x_{6}}{}^{x_{6}}{}^{x_{6}}{}^{x_{6}}{}^{x_{6}}{}^{x_{6}}{}^{x_{6}}{}^{x_{6}}{}^{x_{6}}{}^{x_{6}}{}^{x_{6}}{}^{x_{6}}{}^{x_{6}}{}^{x_{6}}{}^{x_{6}}{}^{x_{6}}{}^{x_{6}}{}^{x_{6}}{}^{x_{6}}{}^{x_{6}}{}^{x_{6}}{}^{x_{6}}{}^{x_{6}}{}^{x_{6}}{}^{x_{6}}{}^{x_{6}}{}^{x_{6}}{}^{x_{6}}{}^{x_{6}}{}^{x_{6}}{}^{x_{6}}{}^{x_{6}}{}^{x_{6}}{}^{x_{6}}{}^{x_{6}}{}^{x_{6}}{}^{x_{6}}{}^{x_{6}}{}^{x_{6}}{}^{x_{6}}{}^{x_{6}}{}^{x_{6}}{}^{x_{6}}{}^{x_{6}}{}^{x_{6}}{}^{x_{6}}{}^{x_{6}}{}^{x_{6}}{}^{x_{6}}{}^{x_{6}}{}^{x_{6}}{}^{x_{6}}{}^{x_{6}}{}^{x_{6}}{}^{x_{6}}{}^{x_{6}}{}^{x_{6}}{}^{x_{6}}{}^{x_{6}}{}^{x_{6}}{}^{x_{6}}{}^{x_{6}}{}^{x_{6}}{}^{x_{6}}{}^{x_{6}}{}^{x_{6}}{}^{x_{6}}{}^{x_{6}}{}^{x_{6}}{}^{x_{6}}{}^{x_{6}}{}^{x_{6}}{}^{x_{6}}{}^{x_{6}}{}^{x_{6}}{}^{x_{6}}{}^{x_{6}}{}^{x_{6}}{}^{x_{6}}{}^{x_{6}}{}^{x_{6}}{}^{x_{6}}{}^{x_{6}}{}^{x_{6}}{}^{x_{6}}{}^{x_{6}}{}^{x_{6}}{}^{x_{6}}{}^{x_{6}}{}^{x_{6}}{}^{x_{6}}{}^{x_{6}}{}^{x_{6}}{}^{x_{6}}{}^{x_{6}}{}^{x_{6}}{}^{x_{6}}{}^{x_{6}}{}^{x_{6}}{}^{x_{6}}{}^{x_{6}}{}^{x_{6}}{}^{x_{6}}{}^{x_{6}}{}^{x_{6}}{}^{x_{6}}{}^{x_{6}}{}^{x_{6}}{}^{x_{6}}{}^{x_{6}}{}^{x_{6}}{}^{x_{6}}{}^{x_{6}}{}^{x_{6}}{}^{x_{6}}{}^{x_{6}}{}^{x_{6}}{}^{x_{6}}{}^{x_{6}}{}^{x_{6}}{}^{x_{6}}{}^{x_{6}}{}^{x_{6}}{}^{x_{6}}{}^{x_{6}}{}^{x_{6}}{}^{x_{6}}{}^{x_{6}}{}^{x_{6}}{}^{x_{6}}{}^{x_{6}}{}^{x_{6}}{}^{x_{6}}{}^{x_{6}}{}^{x_{6}}{}^{x_{6}}{}^{x_{6}}{}^{x_{6}}{}^{x_{6}}{}^{x_{6}}{}^{x_{6}}{}^{x_{6}}{}^{x_{6}}{}^{x_$ | .13 0.32                                                                              | 0.23 0.32                                                                             | .44 0.32                                                                              |
|---------------------------------------------------------------------------------------------------------------------------------------------------------------------------------------------------------------------------------------------------------------------------------------------------------------------------------------------------------------------------------------------------------------------------------------------------------------------------------------------------------------------------------------------------------------------------------------------------------------------------------------------------------------------------------------------------------------------------------------------------------------------------------------------------------------------------------------------------------------------------------------------------------------------------------------------------------------------------------------------------------------------------------------------------------------------------------------------------------------------------------------------------------------------------------------------------------------------------------------------------------------------------------------------------------------------------------------------------------------------------------------------------------------------------------------------------------------------------------------------------------------------------------------------------------------------------------------------------------------------------------------------------------------------------------------------------------------------------------------------------------------------------------------------------------------------------------------------------------------------------------------------------------------------------------------------------------------------------------------------------------------------------------------------------------------------------------------------------------------------------------------------------|---------------------------------------------------------------------------------------|---------------------------------------------------------------------------------------|---------------------------------------------------------------------------------------|
| , y, s                                                                                                                                                                                                                                                                                                                                                                                                                                                                                                                                                                                                                                                                                                                                                                                                                                                                                                                                                                                                                                                                                                                                                                                                                                                                                                                                                                                                                                                                                                                                                                                                                                                                                                                                                                                                                                                                                                                                                                                                                                                                                                                                            | 2.10                                                                                  | 2.10 (                                                                                | 2.10 7                                                                                |
| $\frac{y_{H_2}}{y_{\infty}} \frac{y_{\infty_2}}{y_{H_2}o}$                                                                                                                                                                                                                                                                                                                                                                                                                                                                                                                                                                                                                                                                                                                                                                                                                                                                                                                                                                                                                                                                                                                                                                                                                                                                                                                                                                                                                                                                                                                                                                                                                                                                                                                                                                                                                                                                                                                                                                                                                                                                                        | 131 .0373 .1070 .0129 1.71×10 <sup>-3</sup> 0.41 3.71×10 <sup>-1</sup> 2.10 1.13 0.32 | 075 .0232 .0595 .0008 4.99x10 <sup>-4</sup> 0.41 2.06x10 <sup>-1</sup> 2.10 0.23 0.32 | 023 .0084 .0229 .0039 5.50x10 <sup>-5</sup> 0.41 8.74x10 <sup>-2</sup> 2.10 7.44 0.32 |
| k <sub>4</sub> atm                                                                                                                                                                                                                                                                                                                                                                                                                                                                                                                                                                                                                                                                                                                                                                                                                                                                                                                                                                                                                                                                                                                                                                                                                                                                                                                                                                                                                                                                                                                                                                                                                                                                                                                                                                                                                                                                                                                                                                                                                                                                                                                                | 0.41                                                                                  | 0.41                                                                                  | 0.41                                                                                  |
| $\frac{y_{\rm H_2}}{y_{\rm H_2O}}$                                                                                                                                                                                                                                                                                                                                                                                                                                                                                                                                                                                                                                                                                                                                                                                                                                                                                                                                                                                                                                                                                                                                                                                                                                                                                                                                                                                                                                                                                                                                                                                                                                                                                                                                                                                                                                                                                                                                                                                                                                                                                                                | 1.71×10 <sup>-3</sup>                                                                 | 4.99x10 <sup>-4</sup>                                                                 | 5.50x10 <sup>-5</sup>                                                                 |
| ${}^{\rm Y}_{\rm CH}$                                                                                                                                                                                                                                                                                                                                                                                                                                                                                                                                                                                                                                                                                                                                                                                                                                                                                                                                                                                                                                                                                                                                                                                                                                                                                                                                                                                                                                                                                                                                                                                                                                                                                                                                                                                                                                                                                                                                                                                                                                                                                                                             | .0129                                                                                 | .0008                                                                                 | • 0039                                                                                |
| $^{ m Y}_{ m H_2}$                                                                                                                                                                                                                                                                                                                                                                                                                                                                                                                                                                                                                                                                                                                                                                                                                                                                                                                                                                                                                                                                                                                                                                                                                                                                                                                                                                                                                                                                                                                                                                                                                                                                                                                                                                                                                                                                                                                                                                                                                                                                                                                                | .1070                                                                                 | .0595                                                                                 | .0229                                                                                 |
| $\infty$ $^{y}$ $\infty$ $^{y}$ $^{H}$ $^{z}$ $^{y}$ CH $^{4}$                                                                                                                                                                                                                                                                                                                                                                                                                                                                                                                                                                                                                                                                                                                                                                                                                                                                                                                                                                                                                                                                                                                                                                                                                                                                                                                                                                                                                                                                                                                                                                                                                                                                                                                                                                                                                                                                                                                                                                                                                                                                                    | .0373                                                                                 | .0232                                                                                 | .0084                                                                                 |
| 8 <sub>8</sub>                                                                                                                                                                                                                                                                                                                                                                                                                                                                                                                                                                                                                                                                                                                                                                                                                                                                                                                                                                                                                                                                                                                                                                                                                                                                                                                                                                                                                                                                                                                                                                                                                                                                                                                                                                                                                                                                                                                                                                                                                                                                                                                                    | .0131                                                                                 | .0075                                                                                 |                                                                                       |
| $^{Y}_{N_2}$                                                                                                                                                                                                                                                                                                                                                                                                                                                                                                                                                                                                                                                                                                                                                                                                                                                                                                                                                                                                                                                                                                                                                                                                                                                                                                                                                                                                                                                                                                                                                                                                                                                                                                                                                                                                                                                                                                                                                                                                                                                                                                                                      | .8202 .0094 .01                                                                       |                                                                                       | . 9568 . 0058 . 0                                                                     |
| Y <sub>H2</sub> 0                                                                                                                                                                                                                                                                                                                                                                                                                                                                                                                                                                                                                                                                                                                                                                                                                                                                                                                                                                                                                                                                                                                                                                                                                                                                                                                                                                                                                                                                                                                                                                                                                                                                                                                                                                                                                                                                                                                                                                                                                                                                                                                                 | .8202                                                                                 | .8951 .0130                                                                           | . 9568                                                                                |
| Space<br>Velocity Y <sub>H2</sub> O Y <sub>N2</sub><br>s-1                                                                                                                                                                                                                                                                                                                                                                                                                                                                                                                                                                                                                                                                                                                                                                                                                                                                                                                                                                                                                                                                                                                                                                                                                                                                                                                                                                                                                                                                                                                                                                                                                                                                                                                                                                                                                                                                                                                                                                                                                                                                                        | 2.0                                                                                   | 3.6                                                                                   | 7.3                                                                                   |

TABLE 6.—Average outlet gas compositions for the steam partial pressure experiments at 625°C and space velocity of 4 s<sup>-1</sup>. 0.32 0.32 .5139 .0080 .0106 .0286 .0039 5.26x10<sup>-4</sup> 0.41 8.71x10<sup>-2</sup> 2.10 4.77 0.32 .0042 .0150 .0308 .0057 2.19x10-4 0.41 1.86x10<sup>-1</sup> 2.10 6.01 0.32 4.85x10<sup>-4</sup> 0.41 2.01x10<sup>-1</sup> 2.10 ---2.10 0.23 .0008 4.99x10<sup>-4</sup> 0.41 2.06x10<sup>-1</sup> Y<sub>H2</sub>0  $^{
m Y_{H_2}}$   $^{
m Y_{\infty}}$  $^{
m Y_{CH}}_{f 4}$ .8003 .1172 .0073 .0221 .0532 .0595  $^{Y}_{H_2}$  $^{y}$  $^{\infty}$  $^{y}$  $^{\infty}$ .0232 .0075 .3549 .0130  $^{\rm Y}_{\rm H_2}$ 0  $^{\rm Y}_{\rm N_2}$ .5904 .4351 .8951 Pressure Partial Steam 46 63 83 100

| 100                                                                                                        | ون ا                                                                                                                                                                                                                                                                                                                                                                                                                                                                                                                                                                                                                                                                                                                                                                                                                                                                                                                                                                                                                                                                                                                                                                                                                                                                                                                                                                                                                                                                                                                                                                                                                                                                                                                                                                                                                                                                                                                                                                                                                                                                                                                                                                                                                                                                                                                                                                                                                                                                                        | 12                                                                                      | 32                                                                                      | 19                                                         |
|------------------------------------------------------------------------------------------------------------|---------------------------------------------------------------------------------------------------------------------------------------------------------------------------------------------------------------------------------------------------------------------------------------------------------------------------------------------------------------------------------------------------------------------------------------------------------------------------------------------------------------------------------------------------------------------------------------------------------------------------------------------------------------------------------------------------------------------------------------------------------------------------------------------------------------------------------------------------------------------------------------------------------------------------------------------------------------------------------------------------------------------------------------------------------------------------------------------------------------------------------------------------------------------------------------------------------------------------------------------------------------------------------------------------------------------------------------------------------------------------------------------------------------------------------------------------------------------------------------------------------------------------------------------------------------------------------------------------------------------------------------------------------------------------------------------------------------------------------------------------------------------------------------------------------------------------------------------------------------------------------------------------------------------------------------------------------------------------------------------------------------------------------------------------------------------------------------------------------------------------------------------------------------------------------------------------------------------------------------------------------------------------------------------------------------------------------------------------------------------------------------------------------------------------------------------------------------------------------------------|-----------------------------------------------------------------------------------------|-----------------------------------------------------------------------------------------|------------------------------------------------------------|
| of.                                                                                                        | *                                                                                                                                                                                                                                                                                                                                                                                                                                                                                                                                                                                                                                                                                                                                                                                                                                                                                                                                                                                                                                                                                                                                                                                                                                                                                                                                                                                                                                                                                                                                                                                                                                                                                                                                                                                                                                                                                                                                                                                                                                                                                                                                                                                                                                                                                                                                                                                                                                                                                           | 1.                                                                                      | o                                                                                       | 0.                                                         |
| artial                                                                                                     | $\frac{\mathrm{Y_{CH}_4}}{\mathrm{Y_{H_2}^2}}$                                                                                                                                                                                                                                                                                                                                                                                                                                                                                                                                                                                                                                                                                                                                                                                                                                                                                                                                                                                                                                                                                                                                                                                                                                                                                                                                                                                                                                                                                                                                                                                                                                                                                                                                                                                                                                                                                                                                                                                                                                                                                                                                                                                                                                                                                                                                                                                                                                              | 31.9                                                                                    | 0.23                                                                                    |                                                            |
| team p                                                                                                     | k<br>5                                                                                                                                                                                                                                                                                                                                                                                                                                                                                                                                                                                                                                                                                                                                                                                                                                                                                                                                                                                                                                                                                                                                                                                                                                                                                                                                                                                                                                                                                                                                                                                                                                                                                                                                                                                                                                                                                                                                                                                                                                                                                                                                                                                                                                                                                                                                                                                                                                                                                      | 3,38                                                                                    | 2.10                                                                                    | 1.64                                                       |
| s at s                                                                                                     | $^{Y}_{\infty_2}$                                                                                                                                                                                                                                                                                                                                                                                                                                                                                                                                                                                                                                                                                                                                                                                                                                                                                                                                                                                                                                                                                                                                                                                                                                                                                                                                                                                                                                                                                                                                                                                                                                                                                                                                                                                                                                                                                                                                                                                                                                                                                                                                                                                                                                                                                                                                                                                                                                                                           | K10-2                                                                                   | K10 <sup>-1</sup>                                                                       | к10 <sup>–1</sup>                                          |
| iment                                                                                                      | $\frac{v_{\rm H_2}}{v_{\rm CO}}$                                                                                                                                                                                                                                                                                                                                                                                                                                                                                                                                                                                                                                                                                                                                                                                                                                                                                                                                                                                                                                                                                                                                                                                                                                                                                                                                                                                                                                                                                                                                                                                                                                                                                                                                                                                                                                                                                                                                                                                                                                                                                                                                                                                                                                                                                                                                                                                                                                                            | 2.103                                                                                   | 2.06                                                                                    | 4.173                                                      |
| exper                                                                                                      | k4                                                                                                                                                                                                                                                                                                                                                                                                                                                                                                                                                                                                                                                                                                                                                                                                                                                                                                                                                                                                                                                                                                                                                                                                                                                                                                                                                                                                                                                                                                                                                                                                                                                                                                                                                                                                                                                                                                                                                                                                                                                                                                                                                                                                                                                                                                                                                                                                                                                                                          | 0.13                                                                                    | 0.41                                                                                    | 1.63                                                       |
| t gas compositions for the temperature experiments at steam partial of 100 velocity of 4 s <sup>-1</sup> . | $^{y}$ $\infty$ $^{y}$ $\infty$ $^{y}$ $^{$ | .0006 .0022 .0056 .0010 3.43×10 <sup>-6</sup> 0.13 2.10×10 <sup>-2</sup> 3.38 31.9 1.12 | .0075 .0232 .0595 .0008 4.99x10 <sup>-4</sup> 0.41 2.06x10 <sup>-1</sup> 2.10 0.23 0.32 | 3.06x10 <sup>-3</sup> 1.63 4.17x10 <sup>-1</sup> 1.64 0.19 |
| or the                                                                                                     | Y <sub>CH</sub>                                                                                                                                                                                                                                                                                                                                                                                                                                                                                                                                                                                                                                                                                                                                                                                                                                                                                                                                                                                                                                                                                                                                                                                                                                                                                                                                                                                                                                                                                                                                                                                                                                                                                                                                                                                                                                                                                                                                                                                                                                                                                                                                                                                                                                                                                                                                                                                                                                                                             | .0010                                                                                   | .0008                                                                                   | 1                                                          |
| tions fo<br>4 s <sup>-1</sup> .                                                                            | $^{ m Y}_{ m H_2}$                                                                                                                                                                                                                                                                                                                                                                                                                                                                                                                                                                                                                                                                                                                                                                                                                                                                                                                                                                                                                                                                                                                                                                                                                                                                                                                                                                                                                                                                                                                                                                                                                                                                                                                                                                                                                                                                                                                                                                                                                                                                                                                                                                                                                                                                                                                                                                                                                                                                          | 9500.                                                                                   | .0595                                                                                   | .1248                                                      |
| compositity of 4                                                                                           | $^{y}\omega_{2}$                                                                                                                                                                                                                                                                                                                                                                                                                                                                                                                                                                                                                                                                                                                                                                                                                                                                                                                                                                                                                                                                                                                                                                                                                                                                                                                                                                                                                                                                                                                                                                                                                                                                                                                                                                                                                                                                                                                                                                                                                                                                                                                                                                                                                                                                                                                                                                                                                                                                            | .0022                                                                                   | .0232                                                                                   | .0194 .0513 .1248                                          |
| et gas<br>e veloc                                                                                          | χ                                                                                                                                                                                                                                                                                                                                                                                                                                                                                                                                                                                                                                                                                                                                                                                                                                                                                                                                                                                                                                                                                                                                                                                                                                                                                                                                                                                                                                                                                                                                                                                                                                                                                                                                                                                                                                                                                                                                                                                                                                                                                                                                                                                                                                                                                                                                                                                                                                                                                           | 9000•                                                                                   | .0075                                                                                   | .0194                                                      |
| Average outlet<br>kPa and space                                                                            | $^{Y}_{N_2}$                                                                                                                                                                                                                                                                                                                                                                                                                                                                                                                                                                                                                                                                                                                                                                                                                                                                                                                                                                                                                                                                                                                                                                                                                                                                                                                                                                                                                                                                                                                                                                                                                                                                                                                                                                                                                                                                                                                                                                                                                                                                                                                                                                                                                                                                                                                                                                                                                                                                                | .0123                                                                                   | .0130                                                                                   | .0125                                                      |
| TABLE 7.—Average outlet<br>kPa and space                                                                   | Y <sub>H2</sub> O Y <sub>N2</sub>                                                                                                                                                                                                                                                                                                                                                                                                                                                                                                                                                                                                                                                                                                                                                                                                                                                                                                                                                                                                                                                                                                                                                                                                                                                                                                                                                                                                                                                                                                                                                                                                                                                                                                                                                                                                                                                                                                                                                                                                                                                                                                                                                                                                                                                                                                                                                                                                                                                           | .9782 .0123                                                                             | .8951                                                                                   | .7920 .0125                                                |
| TABLE 7.                                                                                                   | Temper-<br>ature<br>°C                                                                                                                                                                                                                                                                                                                                                                                                                                                                                                                                                                                                                                                                                                                                                                                                                                                                                                                                                                                                                                                                                                                                                                                                                                                                                                                                                                                                                                                                                                                                                                                                                                                                                                                                                                                                                                                                                                                                                                                                                                                                                                                                                                                                                                                                                                                                                                                                                                                                      | 550                                                                                     | 625                                                                                     | 685                                                        |

#### MODELING

In order to predict the rate of gasification of particles of wood char, a model is developed. Wood is composed of an orderly arrangement of small cells called tracheids which are approximately cylinderical in shape (Figure 3). There are essentially two sizes of cells as can be seen in Figure 3. The wood is modeled as a one dimensional flat plate composed of parallel cylinders. It is assumed that mass transfer occurs perpendicular to the plate and that the system is isothermal. All cells are considered to have the same length which is the thickness of the flat plate. The diameter of the cells varies according to a size distribution.

The cells have a length of L = 21, inner radius of r, and an outer radius of R as shown in Figure 14. Steam is transported by convection from the bulk fluid to the cell mouth. Diffusion of steam occurs in the axial direction within the cell. It is assumed that there are no concentration gradients in the radial direction of the cell. As the steam diffuses into the cell the gasification reaction takes place at the wall. The mass is

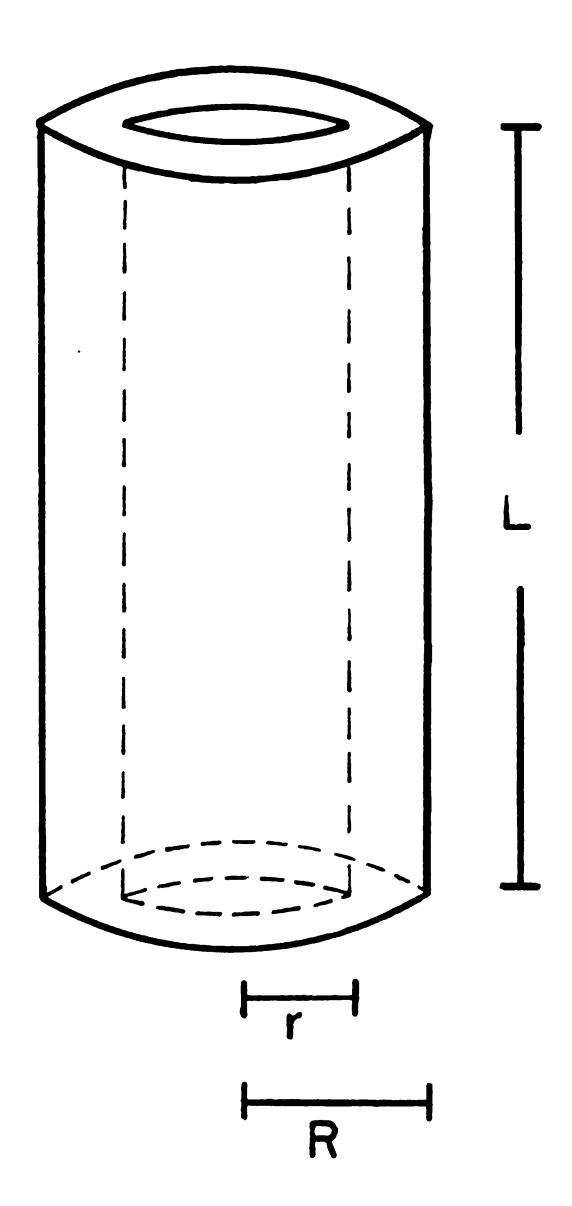


Figure 14.--Diagram of model cell.

consumed and the radius increases. Using these assumptions the following equations are derived.

Mole Balance on Steam:

$$-\pi r^2 \left. D \frac{\partial c}{\partial x} \right|_{x} + \pi r^2 \left. D \frac{\partial c}{\partial x} \right|_{x+\Delta x} - \pi \left( R^2 - r_0^2 \right) \rho \Delta x \text{ rate } = \frac{\partial \pi r^2 c \Delta x}{\partial t}$$
 (16)

$$D r^{2} \frac{\partial^{2} c}{\partial x^{2}} - R_{0} \rho \text{ rate} = 2 cr \frac{\partial r}{\partial t} + r^{2} \frac{\partial c}{\partial t}$$
 (16a)

Mass Balance on Carbon in the Cell Wall:

-rate 
$$\pi(R^2 - r_0^2) \Delta x \rho = \frac{\partial}{\partial t} (\pi R^2 \Delta x - \pi r^2 \Delta x) \rho$$
 (17)

rate 
$$\rho R_{o} = 2r \frac{\partial r}{\partial t}$$
 (17a)

An expression for the reaction rate can be derived using an adsorption-desorption mechanism. This mechanism is described by Equations 18, 19, and 20.

$$H_{2}O \xrightarrow{j_{1}} (H)(OH) \xrightarrow{j_{3}} (O) (H_{2})$$
 (18)

$$H_{2} \stackrel{j_{4}}{\overleftarrow{J}_{5}} (H_{2})$$
(19)

$$C + (0) \xrightarrow{j_6} CO$$
 (20)

If a steady state is assumed and  $\theta_1$ ,  $\theta_2$ , and  $\theta_3$  are the fraction of the active sites covered by (H)(OH), (O), and (H<sub>2</sub>) respectively, the mechanism can be described by Equations 21, 22, and 23 where  $j_6\theta_2$  is the rate of production of carbon monoxide.

$$j_1 p_{H_2O} (1 - \theta_1 - \theta_2 - \theta_3) = (j_2 + j_3)\theta_1$$
 (21)

$$j_3\theta_1 = j_6\theta_2 \tag{22}$$

$$j_3\theta_1 + j_4 p_{H_2} = j_5\theta_3$$
 (23)

Elimination of  $\theta_1$ ,  $\theta_2$ ,  $\theta_3$  leads to the following rate expression (Equation 24).

rate = 
$$\frac{k_1 p_{H_20} - k_3 p_{H_20} p_{H_2}}{1 + k_2 p_{H_20}}$$
 (24)

Equations 25, 26, and 27 give expressions for the k's in terms of the j's.

$$k_1 = \frac{j_3}{j_6(j_2 + j_3)}$$
 (25)

$$K_{2} = \frac{\hat{j}_{3}(1 + \frac{\hat{j}_{6}}{\hat{j}_{3}} + \frac{\hat{j}_{6}}{\hat{j}_{5}})}{\hat{k}_{2} = \frac{\hat{j}_{3}(1 + \frac{\hat{j}_{6}}{\hat{j}_{3}} + \frac{\hat{j}_{6}}{\hat{j}_{5}})}{\hat{j}_{6}(\hat{j}_{2} + \hat{j}_{3})} \times (26)$$

$$k_{3} = \frac{j_{3} j_{4}}{25(32+63)} \times k_{3} = \frac{j_{3} j_{4}}{j_{6} j_{5} (j_{2} + j_{3})} \times (27)$$

Equations 16a and 17a can be solved simultaneously to give the steam concentration and the inner radius of the cell as a function of length and time. This is a rigorous model which can be simplified with some assumptions.

It was assumed that the change in the radius during reaction was small compared to the total radius so r was considered to be constant. Only the steady state solution was considered so the concentration was only a function of length. First order kinetics, Equation 13, were used in this analysis and the rate constant was based on the experimental data of this study. These assumptions lead to the following differential equation (Equation 28).

$$r^2 D \frac{\partial^2 c}{\partial x^2} = -R_0 \rho k' / C \qquad (28)$$

B.C. 1 at 
$$x = 0$$
,  $\frac{\partial c}{\partial x} = 0$  (28a)

B.C. 2 at 
$$x = l$$
,  $c = c_0$  (28b)

The above equations are transformed into dimensionless variables and yield Equations 29, 29a, and 29b.

$$\frac{\partial^2 \psi}{\partial \xi^2} = \phi^2 \psi \tag{29}$$

B.C. 1 at 
$$\xi = 0$$
,  $\frac{\partial \psi}{\partial \xi} = 0$  (29a)

B.C. 2 at 
$$\xi = 1$$
,  $\psi = 1$  (29b)

The second boundary condition was chosen based on the experimental evidence that the reaction is essentially independent of space velocity. Since these experiments indicated that external mass transfer was not controlling, the concentration at the char surface was assumed to be the concentration in the bulk fluid (Equation 28b).

An isothermal effectiveness factor was calculated (Equation 30) for two cell sizes and is shown in Figure 15 as a function of cell length.

$$\eta = \frac{\tanh \phi}{\phi} \tag{30}$$

 $\eta_L$  and  $\eta_S$  are the isothermal effectiveness factors for the large and small cells respectively. The cells have inner radii of 35  $\mu m$  and 10  $\mu m$  and there are 3000 cells/cm² and and 232,500 cells/cm², respectively. Using this distribution the isothermal effectiveness factor of the char is essentially that of the small cells.

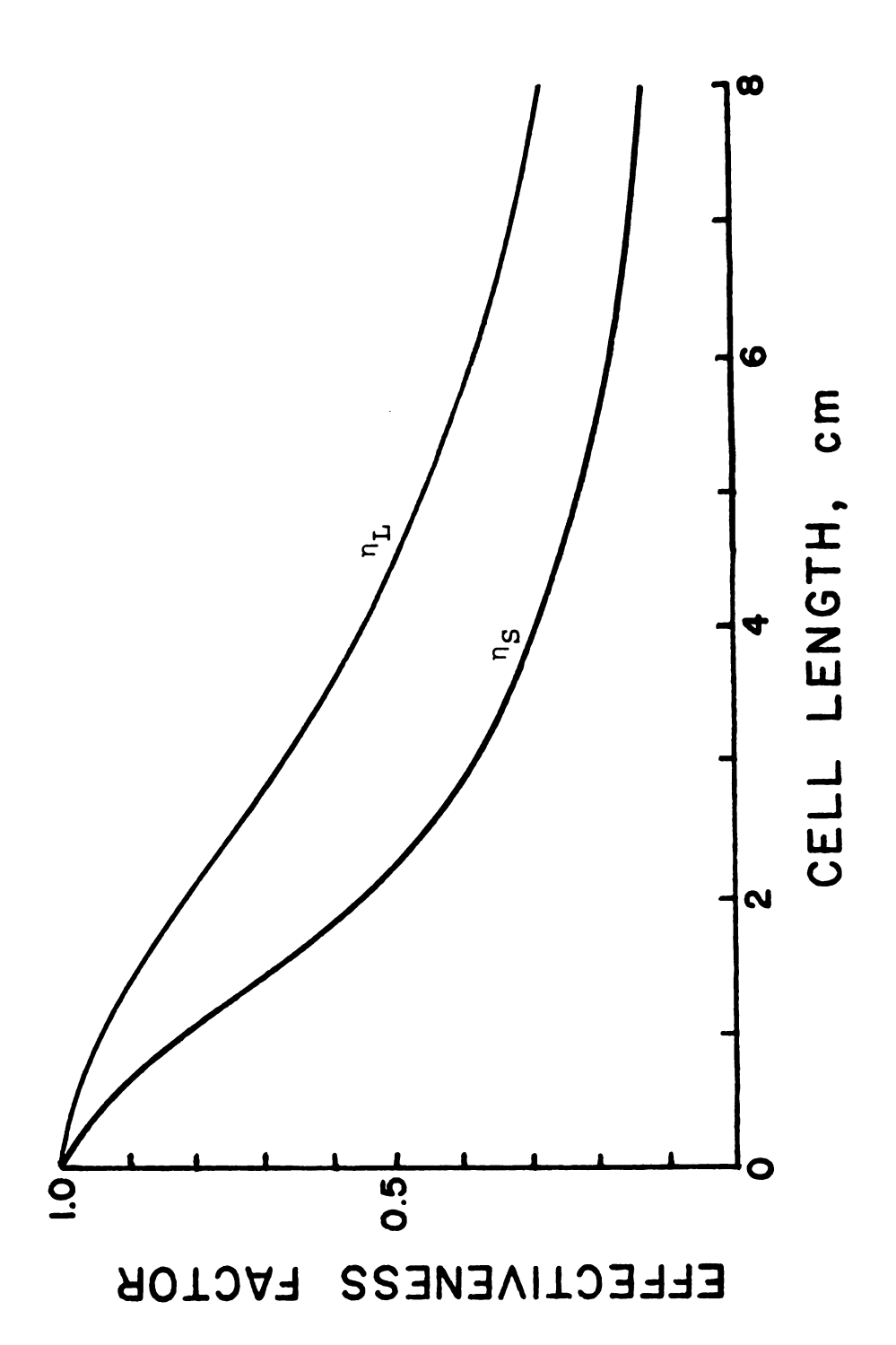


Figure 15.--Isothermal effectiveness factor versus cell length for gasification of Poplar SPP char at 625°C.

### CONCLUSIONS

A study was conducted to determine the kinetics of gasification of wood char. Poplar SPP was ground to a uniform size and pyrolyzed at 700°C in nitrogen for 10 minutes to produce the char. The effects of temperature, steam partial pressure, and space velocity on the gasification rate were determined.

The product gas of gasification was composed of carbon dioxide, carbon monoxide, hydrogen, and methane. It was not known if the methane was produced directly from the char or from the carbon monoxide. In a study on the gasification of coconut char Blackwood and McGrory (5) speculated that the methane was formed from the reaction of steam or hydrogen with -CH<sub>2</sub> groups on the carbon surface. Another possible source of methane was from the catalytic reaction of hydrogen with carbon monoxide. Because of these two possible sources of methane the experimental gasification rate was calculated for two cases.

In Case I the gasification rate was calculated from the carbon in the carbon oxides of the product gas. The gasification rate expression was determined to be

first order with respect to steam. The rate constant was found to be  $3.74 \times 10^{-5} \, \text{mol/min}$  g kPa and the activation energy was 156 kJ/mol. The measured rate decreased with increasing space velocity. This behavior was attributed to experimental error and not an effect of space velocity which indicates that the reaction was not externally mass transfer controlled.

In Case II the gasification rate was calculated from the carbon in the carbon oxides plus the methane. The data was found to fit a Langmuir type of rate expression with  $k_1$  and  $k_2$  being  $8.203 \times 10^{-5}$  mol/min g kPa and  $1.315 \times 10^{-2}$  kPa<sup>-1</sup> respectively. This type of expression was predicted by an adsorption-desorption mechanism. The better fit of the data for the second model indicates that the methane was probably produced from the carbon dioxide. To confirm this more experimentation would be required.

A model was developed for the isothermal effectiveness factor versus particle size using kinetic constants obtained from experiments of this study and estimated diffusivities. This model predicted that diffusion control of the reaction becomes important for particles larger that 0.5 cm. Both external and internal mass transfer resistances were shown to be negligible for the particle sizes and conditions of the experimentation of

this study. Based on these conclusions the rate measurements were used to calculate the intrinsic kinetics.

## RECOMMENDATIONS FOR FUTURE WORK

This study has laid the groundwork for a more in depth study of wood char gasification. In order to better understand the process the following points need to be examined:

- (1) Chemical analysis of the char samples.
- (2) The gasification reactions of pyrolysis products so that gasification of wood instead of wood char can be studied.
- (3) A larger range of temperatures (700°C to 1000°C). A new furnace and controller would be required.
- (4) Higher total pressures so that higher steam partial pressures (2 atm to 10 atm) can be studied. A new reactor and high pressure facilities would be required.
- (5) Various partial pressures at higher temperatures so the activation energies of the Langmuirian rate constants can be determined. No new equipment is required.
- (6) Different particle sizes so that the isothermal effectiveness factor presented in this study can be verified. No new equipment is required.
- (7) Char surface area measurements so that the mechanism of the gasification reaction can be examined. An electrobalance would be required so that the amount of gas adsorption to the char could be measured.

- (8) Effect of other gases, such as hydrogen and carbon monoxide, on the reaction rate. New facilities for adding these gases to the inlet of the reactor would be required.
- (9) Calculation of nonisothermal effectiveness factors.
- (10) Verification of results by making additional temperature and steam partial pressure experiments. No new facilities are required.
- (11) Calculation of isothermal effectiveness factors for Langmuir-Hinshelwood kinetics.

APPENDIX

SAMPLE CALCULATIONS

## SAMPLE CALCULATIONS

The following presents sample calculations for the experimental run with a temperature of 550°C, steam partial pressure of 100 kPa, and a space velocity of  $\mu s^{-1}$ .

Calculation of Product Gas Composition\*

APPENDIX TABLE 1.--Gas chromotograph results.

| Component                    | Calibration<br>Factor, f | Peak Weight, w |
|------------------------------|--------------------------|----------------|
| <sup>H</sup> 2               | 2.41                     | 0.07475        |
| N <sub>2</sub>               | 1.00                     | 0.18703        |
| СО                           | 0.96                     | 0.00600        |
| $\mathtt{CH}_{oldsymbol{4}}$ | 0.82                     | 0.00726        |
| co <sub>2</sub>              | 1.53                     | 0.02826        |

mol fraction<sub>i</sub> = 
$$\frac{f_i w_i}{5}$$

$$c=1$$

$$c=1$$

<sup>\*</sup>The product gas compositions were averaged over all of the gas samples taken. Only the data for one gas sample is presented above.

| APPENDIX | TABLE | 2Gas | sample | compositions. |
|----------|-------|------|--------|---------------|
|          |       |      |        |               |

| Component       | Mol Fraction | Mol Fraction<br>on Nitrogen<br>Free Basis |
|-----------------|--------------|-------------------------------------------|
| <sup>H</sup> 2  | .243         | .618                                      |
| N <sub>2</sub>  | .607         |                                           |
| со              | .019         | .051                                      |
| CH <sub>4</sub> | .039         | .099                                      |
| co <sub>2</sub> | .092         | .234                                      |

# Calculation of Material Balance

Average nitrogen flow = 0.105 1/min at 25°C, 1 atm

Total carbon in product gas = 
$$\frac{\text{Total gas - N}_2 \text{ (1) } | 1.0 \text{ (mol)} | | 12 \text{ (g)}}{| 24.451 \text{ (1) } | 1 \text{ (mol)}}$$

$$\text{x mol fraction of } (\text{CO}_2 + \text{CO} + \text{CH}_4)$$

$$= \frac{1.20 \text{ (1.0) (12) (.238 + .060 + .102)}}{24.451}$$

= 0.24 grams

Total carbon consumed = 0.24 grams

% error = 
$$\frac{\text{Total carbon in product gas - Total carbon consumed}}{\text{Total carbon consumed}}$$
$$= \frac{0.24 - 0.24}{0.24}$$
$$= 0.0%$$

# Calculation of Gasification Rate

rate = Average product gas flow rate (1/min) - average nitrogen flow rate (1/min)
Original carbon present (g)

$$\times \frac{1.0 \text{ mol}}{24.451 \text{ (1)}} | \text{mol fraction of (CO + CO2)}$$

$$= \frac{(0.185 \text{ l/min} - 0.105 \text{ l/min}) (.238 + .060)}{24.451 \text{ l/mol x 2.67 g}}$$

= 
$$3.652 \times 10^{-4} \frac{\text{mol}}{\text{g min}}$$

REFERENCES

#### REFERENCES

- 1. Stamm, Alfred J., Wood and Cellulose Science. New York: The Ronald Press Company, (1964).
- 2. Panshin, A.J., and Carl deZeeuw, <u>Textbook of Wood</u>
  <u>Technology</u>, Vol. 1, 3rd ed. New York: McGrawHill Book Company, (1970).
- 3. Shafizadeh, F., and G.D. McGinnis, "Morphology and Biogenesis of Cellulose and Plant Cell-Walls," Advan. Carbohyd. Chem. Biochem., 26, 297, (1971).
- 4. Browne, F.L., "Theories of the Combustion of Wood and Its Control," Forest Products Laboratory Report No. 2136, (1963).
- 5. Blackwood, J.D., and F. McGrory, "The Carbon-Steam Reaction at High Pressure," Aust. J. Chem., 11, 16, (1958).
- 6. Gregg, D.W., and T.F. Edgar, "Underground Coal Gasification," AIChE J., 24, 5, (1978).
- 7. Graven, W.M., and F.J. Long, "Kinetics and Mechanisms of the Two Opposing Reactions CO +  $H_2O = CO_2 + H_2$ ," Journal ACS, 76, 2602, (1954).
- 8. Blackwood, J.D., "The Kinetics of the System Carbon-Hydrogen-Methane," Aust. J. Chem., 15, 397, (1962).
- 9. Blackwood, J.D., and D.J. McCarthy, and B.D. Cullis, "The Carbon-Hydrogen Reaction with Cokes and Chars," Aust. J. Chem., 20, 2525, (1967).
- 10. Blackwood, J.D., and D.J. McCarthy, and B.D. Cullis, "Reactivity in the System Carbon-Hydrogen-Methane," Aust. J. Chem., 20, 1561, (1967).
- 11. Fischer, J., J.E. Young, R.N. Lo, D.C. Bowyer, J.E. Johnson, and A.A. Jonke, "Gasification of Chars Produced Under Simulated in situ Processing Conditions," ANL-76-131, (1976).

12. Taylor, R.W., and D.W. Bowen, "Rate of Reaction of Steam and Carbon Dioxide with Chars Produced from Subbituminous Coals," UCRL-52002, (1976).

